© 2022. Published by The Company of Biologists Ltd | Journal of Cell Science (2022) 135, jcs259592. doi:10.1242/jcs.259592

RESEARCH ARTICLE

SPECIAL ISSUE: CELL BIOLOGY OF LIPIDS

Analysis of sex-specific lipid metabolism of *Plasmodium falciparum* points to the importance of sphingomyelin for gametocytogenesis

Melanie C. Ridgway[1], Daniela Cihalova[1], Simon H. J. Brown[2], Phuong Tran[1], Todd W. Mitchell[3] and Alexander G. Maier[1,*]

ABSTRACT

Male and female *Plasmodium falciparum* gametocytes are the parasite lifecycle stage responsible for transmission of malaria from the human host to the mosquito vector. Not only are gametocytes able to survive in radically different host environments, but they are also precursors for male and female gametes that reproduce sexually soon after ingestion by the mosquito. Here, we investigate the sex-specific lipid metabolism of gametocytes within their host red blood cell. Comparison of the male and female lipidome identifies cholesteryl esters and dihydrosphingomyelin enrichment in female gametocytes. Chemical inhibition of each of these lipid types in mature gametocytes suggests dihydrosphingomyelin synthesis but not cholesteryl ester synthesis is important for gametocyte viability. Genetic disruption of each of the two sphingomyelin synthase genes points towards sphingomyelin synthesis contributing to gametocytogenesis. This study shows that gametocytes are distinct from asexual stages, and that the lipid composition is also vastly different between male and female gametocytes, reflecting the different cellular roles these stages play. Taken together, our results highlight the sex-specific nature of gametocyte lipid metabolism, which has the potential to be targeted to block malaria transmission.

This article has an associated First Person interview with the first author of the paper.

KEY WORDS: Gametocytes, Lipidome, Malaria, *Plasmodium falciparum*, Sphingomyelin, Transmission

INTRODUCTION

Transmission of *Plasmodium falciparum* from the human to mosquito host depends on male and female gametocytes. The development of transmissible gametocytes (gametocytogenesis) is by far the longest developmental sexual stage in *P. falciparum*. After 10–12 days of maturation in the human red blood cell (RBC), ingestion by a mosquito rapidly activates the gametocytes to form mature gametes capable of sexual reproduction (Bennink et al., 2016). Within 15 min of the blood meal, gametocytes egress from their host RBC. While male gametocytes multiply into eight flagellated microgametes, female gametocytes form an immobile spherical macrogamete, poised for fertilisation. The zygote develops in the extracellular environment until invasion of the mosquito midgut wall 19–36 h post blood meal (Aikawa et al., 1984; Sinden et al., 1985; Vlachou et al., 2004).

Such a rapid sex-specific metamorphosis is necessarily preceded by sex-specific preparations in the human host during the relatively slow gametocytogenesis. Surprisingly though, morphological gametocyte sex dimorphism is relatively subtle and mostly limited to the ultrastructural level. Recently, the tagging of sex-specific molecular markers has revealed sex-specific gene and protein expression profiles (Lasonder et al., 2016; Miao et al., 2017). These studies have identified differences in the expression of mRNA and protein involved in lipid metabolic pathways including phosphatidylcholine biosynthesis, fatty acid biosynthesis and ether lipid metabolism (Lasonder et al., 2016). Whether this results in differences in the lipid composition between male and female gametocytes remains unknown.

Lipids fulfil a vast range of functions in the cell. They not only provide building blocks in the form of fatty acids for parasite metabolism, but they also form the basis for membranes (mainly phospholipids and cholesterol), functionalise subdomains within membranes (for example, sphingolipids), serve as energy storage (for example, neutral lipids such as cholesteryl esters and triacylglycerol) and act as signalling molecules (for example, diacylglycerol and ceramide). The nature of lipids in male and female gametocytes may reveal diverging cellular functions that precede sex-specific development in the mosquito.

Based on their resilience against many drugs that are active against asexual forms, gametocytes were generally thought to be relatively metabolically inactive (Canning and Sinden, 1975; Sinden et al., 1978). However, the lipidome of combined male and female gametocytes changes significantly between young and mature gametocytes (Gulati et al., 2015; Tran et al., 2016), suggesting that lipid metabolism is active during gametocytogenesis. In particular, Gulati et al. (2015) have identified intermediate products of sphingolipid metabolism in mature gametocytes, revealing that *de novo* sphingomyelin (SM) synthesis occurs during gametocytogenesis.

SM is synthesised *de novo* from serine and palmitoyl-CoA in five consecutive reactions. The final step of *de novo* SM synthesis is mediated by sphingomyelin synthase (SMS). *P. falciparum* encodes two SMS proteins (Gardner et al., 2002), one of which is expressed throughout blood stages (SMS1; PlasmoDB: PF3D7_0625000), the other of which is gametocyte specific and female enriched (SMS2; PlasmoDB: PF3D7_0625100) (López-Barragán et al., 2011; Lasonder et al., 2016). In addition to generating SM, SMS also

[1]Research School of Biology, Australian National University, Canberra, Australian Capital Territory 2601, Australia. [2]Molecular Horizons and School of Chemistry and Molecular Biology, University of Wollongong, Wollongong, New South Wales 2522, Australia. [3]Illawarra Health and Medical Research Institute and School of Medicine, University of Wollongong, Wollongong, New South Wales 2522, Australia.

*Author for correspondence (alex.maier@anu.edu.au)

T.W.M., 0000-0002-1372-9963; A.G.M., 0000-0001-7369-1058

Handling Editor: Michael Way
Received 16 November 2021; Accepted 18 November 2021

Journal of Cell Science (2022) 135, jcs259592. doi:10.1242/jcs.259592

regulates the levels of secondary messenger molecules such as ceramide and diacylglycerol (Fyrst and Saba, 2010). The functional significance of SMS1 and SMS2 in *P. falciparum* is yet to be investigated.

Here, we explore the sex-specific lipidome of mature *P. falciparum* gametocytes within their host RBC to determine the respective contribution of male and female gametocytes to the lipid profile of the infected RBC (iRBC). The functional significance of *de novo* synthesis of key sex-specific lipids is then investigated using pharmacological inhibition and reverse genetics.

RESULTS

The lipid composition of iRBCs is characteristic of parasite sex and lifecycle stage

Lipidomic analysis was performed on uninfected RBCs and RBCs infected with male gametocytes, female gametocytes or mature asexual blood-stage parasites. Over 230 lipid species were identified in the samples (for a complete list refer to Table S4). We performed a principal component analysis to determine the relative contribution of each of these lipid species to the variation between samples (Fig. 1). The principal component analysis plot (Fig. 1A) groups together samples of similar lipid composition, and the corresponding loading plot (Fig. 1B) illustrates which lipid species distinguish sample groups.

In considering all measured lipids by principal component analysis, the biggest difference in lipid composition distinguishes infected from uninfected RBCs regardless of parasite lifecycle stage [principal component 1 (PC1), Fig. 1A]. A third of the lipid variation between samples nevertheless separates asexual parasite-infected RBCs, male gametocyte-infected RBCs and female gametocyte-infected RBCs [principal component 2 (PC2), Fig. 1A]. Parasite stages mainly cluster based on cholesteryl ester (CE) species, free cholesterol (FC), diacylglycerol (DAG) and phosphatidylcholine (PC) (Fig. 1B).

Female gametocyte-infected RBCs contain more neutral lipids than other stages

Upon infection, total lipid abundance in iRBCs increases 3–5 fold, and in sexual stages, female gametocyte-infected RBCs accumulate significantly more lipids than male gametocyte-infected RBCs (Fig. 1C). However, this increase is not reflected across all lipids: of the four main lipid categories (phospholipids, sphingolipids, free cholesterol and neutral lipids), only neutral lipids are significantly more abundant in female gametocyte-infected RBCs compared to

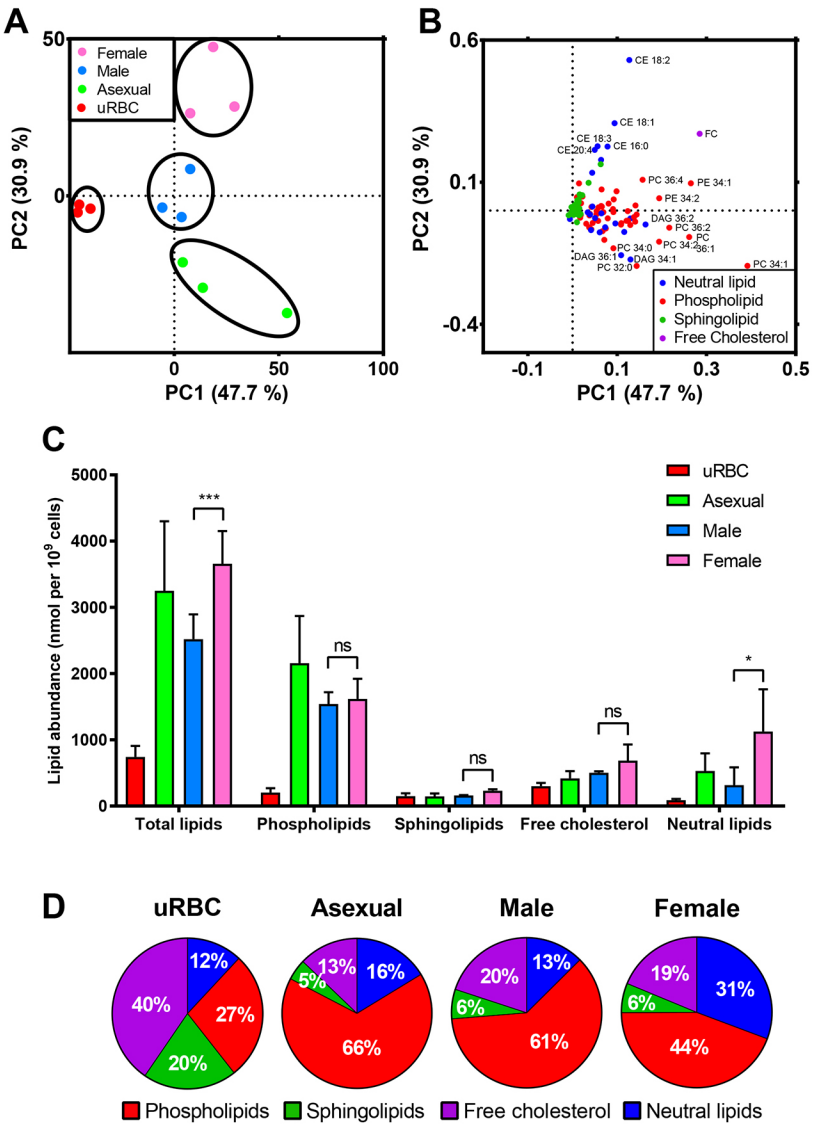

Fig. 1. Overview of the lipidomes of iRBCs and uninfected RBCs. (A,B) Principal component analysis (A) and loading plot (B) of the lipidome of uninfected RBCs (uRBC, red) and RBCs infected with asexual stage parasites (Asexual, green), female gametocytes (Female, pink) and male gametocytes (Male, blue). Black circles in A indicate sample groups, with three independent biological replicates shown as points. The individual lipid species in B are colour-coded to indicate the group they belong to (neutral lipids, blue; phospholipids, red; sphingolipids, green; free cholesterol, indigo). Selected lipid names are shown in B. Percentages for each principal component indicate the contribution of each component to overall variation between samples. (C,D) Mean±s.d. lipid abundance (C) and mean lipid proportions (D) of lipid classes in uRBCs and RBCs infected with asexual stage parasites, male gametocytes and female gametocytes. Results averaged from three independent biological replicates of 10^7 cells each. ***P<0.001; *P<0.1; ns, not significant, P>0.1 (two-way ANOVA with Tukey's post hoc test).

Journal of Cell Science (2022) 135, jcs259592. doi:10.1242/jcs.259592

male gametocyte-infected RBCs (Fig. 1C). This is also reflected in the relative proportions of lipid groups in each stage: neutral lipids account for 31% of lipids in female gametocyte-infected RBCs compared to only 13% in male gametocyte-infected RBCs (Fig. 1D). Sphingolipid and free cholesterol contents are similar in abundance but decrease in relative terms in RBCs upon infection or in sexual stages. Phospholipids, on the other hand, are more abundant and represent a larger proportion of the relative lipid contribution in iRBCs.

In general, neutral lipids are a cellular means of storing energy and contribute to intracellular signalling pathways. The nature of neutral lipids in asexual parasite-infected RBCs contrasts to that of gametocyte-infected RBCs (Fig. 2). Of the three neutral lipids groups [CE, DAG and triacylglycerol (TAG)], DAG and TAG are the predominant neutral lipids in asexual parasite-infected RBCs, whereas CE dominates the neutral lipid profile of gametocyte-infected RBCs and uninfected RBCs (Fig. 2A,B). The proportions of

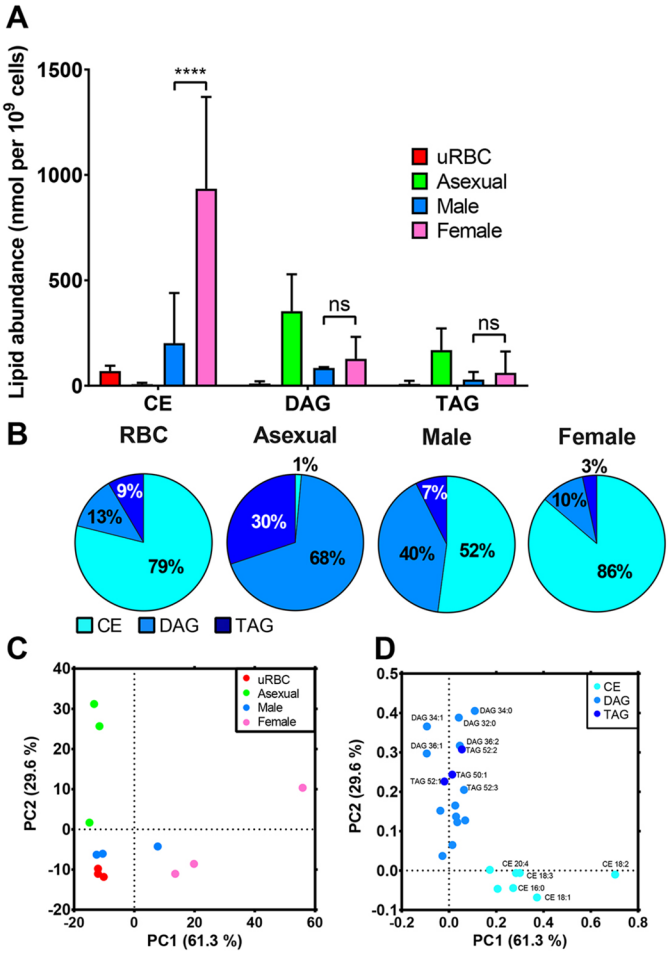

Fig. 2. Analysis of neutral lipids in iRBCs and uninfected RBCs. (A,B) Mean±s.d. neutral lipid abundance (A) and mean neutral lipid proportions (B) of uninfected red blood cells (uRBC) and RBCs infected with asexual-stage parasites, male gametocytes or female gametocytes. Results averaged from three independent biological replicates of 10^7 cells. ****P<0.0001; ns, not significant, P>0.1 (two-way ANOVA with Tukey's post hoc test). (C,D) Principal component analysis (C) and loading plot (D) of neutral lipid composition of uRBCs and RBCs infected with asexual-stage parasites, male gametocytes or female gametocytes. In C, the three independent biological replicates are shown as points. In D, selected neutral lipid names are shown. Percentages for each principal component indicate the contribution of each component to overall variation between samples.

neutral lipid categories are highly dynamic upon infection with asexual- or sexual-stage *P. falciparum*. In addition, accumulation of neutral lipids is sex specific: female gametocyte-infected RBCs accumulate significantly more CE than male gametocyte-infected RBCs (Fig. 2A). These trends are also observed at the individual lipid species level (Fig. 2C,D). CE species characterise female gametocyte-infected RBCs whereas asexual parasite-infected RBCs are distinguished by DAG and TAG species (Fig. 2C,D).

Phospholipids of gametocyte-infected RBCs differ from those of asexual stage parasite-infected RBCs but are not sex specific

Phospholipids are the main component of membranes and, amongst others, are required for organelle biogenesis. Hence it is not surprising that most lipids in iRBCs belong to this group (Fig. 1A). Although male gametocyte-infected RBCs have a higher proportion of phospholipids (61% phospholipids in males compared to 44% in females, Fig. 1D), phospholipid abundance is similar in male and female gametocyte-infected RBCs (Fig. 1C). There were no significant differences in the major phospholipid groups PC, phosphatidyl ethanolamine (PE), phosphatidyl serine (PS) or phosphatidyl glycerol (PG) between sexes (Fig. 3A). PG was only detected in iRBCs. Male gametocyte-infected RBCs contain slightly more PC but slightly less PE than female gametocyte-infected RBCs, both in terms of abundance and proportion of phospholipids (Fig. 3A,B).

Principal component analysis based only on phospholipids does not distinguish between male and female gametocyte-infected RBCs (Fig. 3C). However, gametocyte-infected RBCs cluster apart from uninfected RBCs and asexual parasite-infected RBCs mostly due to the contribution of PE species (Fig. 3C,D). Overall, male and female gametocyte-infected RBC phospholipids are similar to each other but are distinct from host cell and asexual parasite-infected RBC phospholipids.

The sphingolipid dihydrosphingomyelin is a key characteristic of female gametocytes

Sphingolipids are also components of cell membranes and form detergent-resistant lipid domains that are platforms for intracellular signalling. Like phospholipids, overall sphingolipid abundance is not significantly different between male and female gametocyte-infected RBCs (Fig. 1C). However, breaking down sphingolipids into three main groups – SM, dihydrosphingomyelin (DHSM) and ceramide – reveals gametocyte-specific and sex-specific sphingolipid groups (Fig. 4). Unlike the abundance of the major sphingolipid SM, which is similar in all samples (Fig. 4A), gametocyte-infected RBCs (especially female gametocyte-infected RBCs) accumulate DHSM (Fig. 4A,B).

Principal component analysis of sphingolipids alone does not distinguish uninfected RBCs from asexual parasite-infected RBCs. However, male and female gametocyte-infected RBCs cluster separately (Fig. 4C). DHSM 20:0, 16:0 and 18:0 especially distinguish gametocyte-infected RBCs from the other samples (Fig. 4D). Overall, accumulation of DHSM marks gametocytogenesis and is even more pronounced in females.

Of the lipid species with more than a two-fold difference between female and male gametocyte-infected RBCs, six are significantly more abundant in female gametocyte-infected RBCs (Fig. 5A). Five of these are saturated DHSM species (between C16 and C20 in size), the other is SM 22:2, identifying sphingolipids as the major sex-specific lipid group. On average, several neutral lipid species also appear more abundant in female gametocyte-infected

Journal of Cell Science (2022) 135, jcs259592. doi:10.1242/jcs.259592

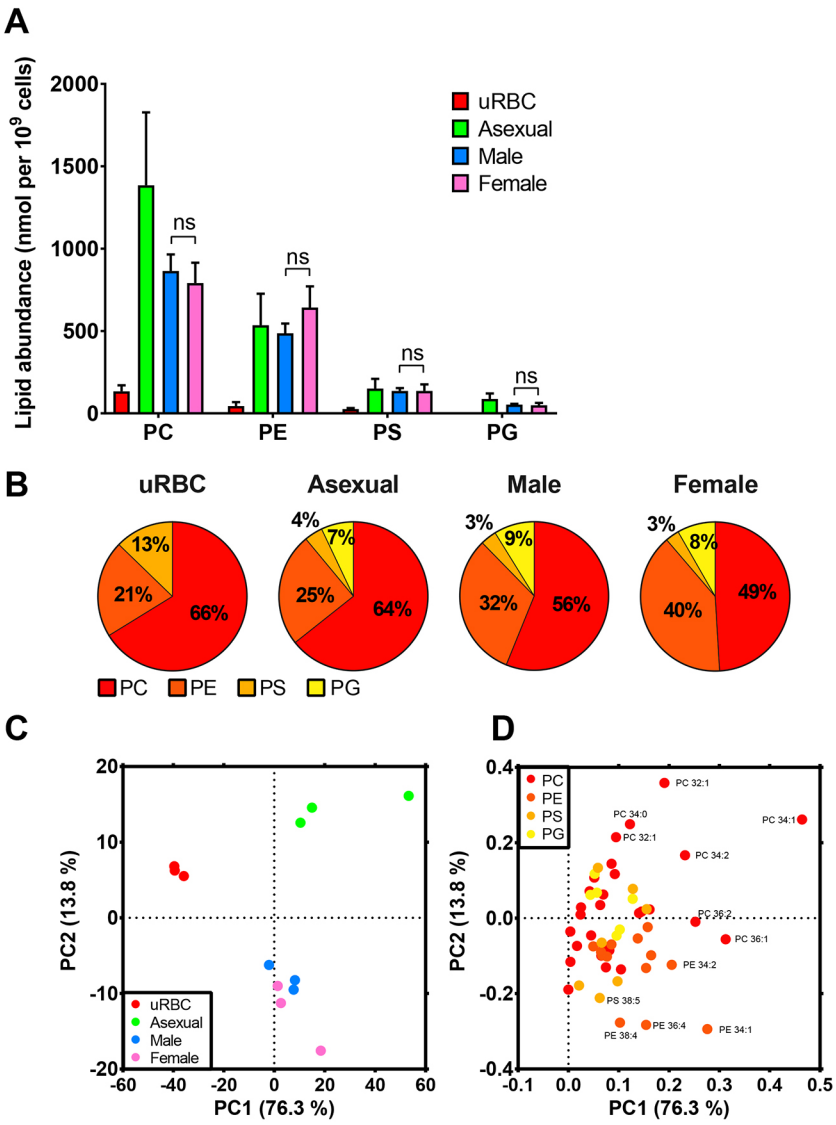

Fig. 3. Analysis of phospholipids in iRBCs and uninfected RBCs. (A,B) Mean±s.d. phospholipid abundance (A) and mean phospholipid proportions (B) of uninfected red blood cells (uRBC) and RBCs infected with asexual-stage parasites, male gametocytes or female gametocytes. Results averaged from three independent biological replicates of 10^7 cells. ns, not significant, P>0.1 (two-way ANOVA with Tukey's post hoc test). (C,D) Principal component analysis (C) and loading plot (D) of phospholipid composition of uRBCs and RBCs infected with asexual-stage parasites, male gametocytes or female gametocytes. In C, the three independent biological replicates are shown as points. In D, selected phospholipid names are shown. Percentages for each principal component indicate the contribution of each component to overall variation between samples.

RBCs; however, this difference lacks statistical significance due to variation between biological replicates. No lipid species are significantly more abundant in male gametocyte-infected RBCs, although some phospholipid species are more abundant on average. Overall, the sex-specific lipid profile of gametocyte-infected RBCs points towards DHSM as a key characteristic of female gametocytes.

Compared to asexual stage parasite-infected RBCs, both sexes of gametocyte-infected RBCs contain more DHSM 20:0, 18:0 and 16:0 (Fig. 5B,C). Asexual parasite-infected RBCs, on the other hand, contain significantly more of some PC species compared to both sexes of gametocyte-infected RBCs [PC32:0, PC32:1, PC34:0 and PC36:0 (in males only)]. CE 16:1 and CE 16:0 are the only lipid species that are more abundant in female gametocyte-infected RBCs but not in male gametocyte-infected RBCs when compared to asexual parasite-infected RBCs, which might point to specialised functions of these lipid species in female parasites. Several phospholipid and sphingolipid species are significantly more abundant in each sex of gametocyte-infected RBCs compared to uninfected RBCs (Fig. 5D,E). Overall, gametocytes significantly modify the lipid profile of the host RBC during maturation in a manner that distinguishes them from asexual parasites.

Sphingolipid synthesis is functionally important in both asexual and sexual blood stages

To investigate the functional significance of the sex-specific lipid composition, gametocytes were exposed to three compounds that block the synthesis of the most sex-specific lipids (CE and sphingolipids) from day 2 to day 6 post commitment (Fig. 6). Thereafter the sex-specific viability of gametocytes was measured using flow cytometry. GT11 is an analogue of dihydroceramide that cannot be metabolised by dihydroceramide desaturase in mammalian cells, thereby blocking the enzyme responsible for ceramide synthesis (Bedia et al., 2005). At concentrations greater than 5 µM, GT11 has been shown to more generally decrease *de novo* sphingolipid synthesis in cultured mammalian cells (Triola et al., 2004). Glibenclamide and Sandoz 58-035 directly inhibit cholesterol esterification by acyl-coenzyme A:cholesterol acyltransferase in mammalian cells (Ross et al., 1984). At 10 µM, only the sphingolipid synthesis inhibitor GT11 appears to impact gametocyte viability in a male-specific manner (Fig. 6).

The apparent sex-specific function of sphingolipid synthesis in gametocytes was further investigated using reverse genetics. DHSM and SM are synthesised by SMS from dihydroceramide and ceramide, respectively. *P. falciparum* encodes two such enzymes,

Journal of Cell Science (2022) 135, jcs259592. doi:10.1242/jcs.259592

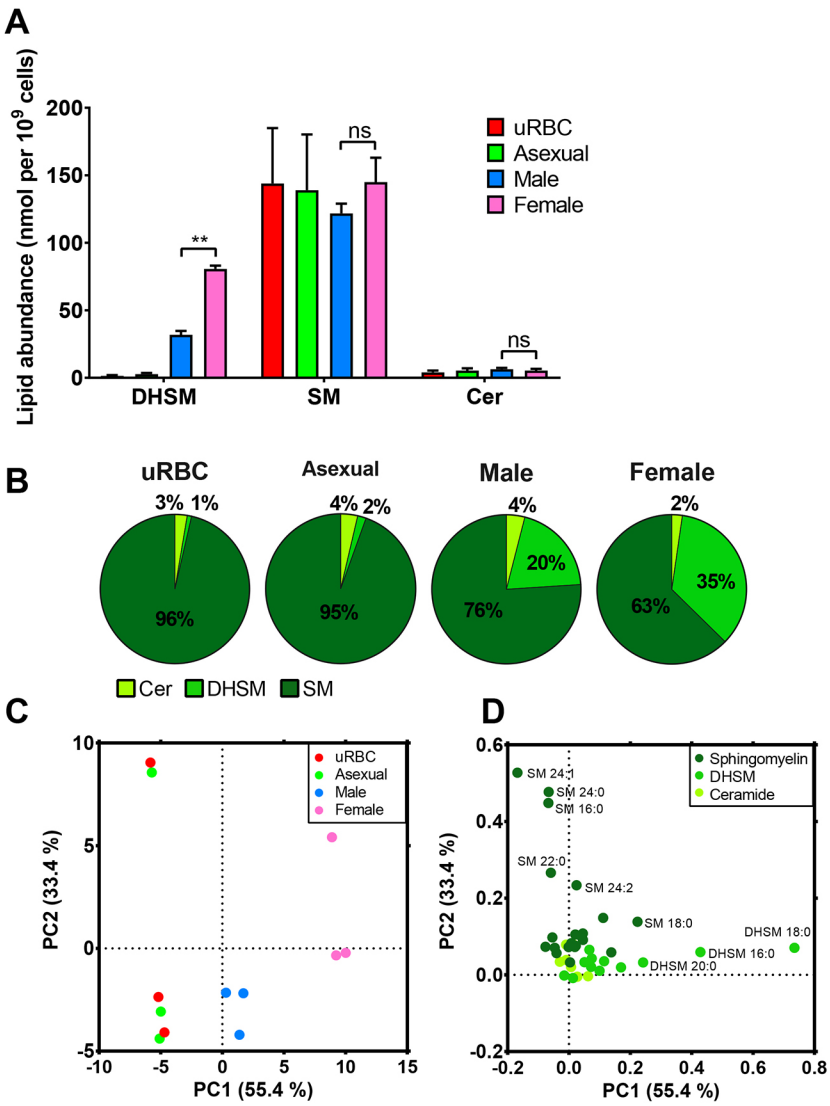

Fig. 4. Analysis of sphingolipids in iRBCs and uninfected RBCs. (A,B) Mean±s.d. sphingolipid abundance (A) and mean sphingolipid proportions (B) of uninfected red blood cells (uRBC) and RBCs infected with asexual stage parasites male gametocytes or female gametocytes. Results averaged from three independent biological replicates of 10^7 cells. $^{**}P<0.01$; ns, not significant, $P>0.1$ (two-way ANOVA with Tukey's post hoc test). (C,D) Principal component analysis (C) and loading plot (D) of sphingolipid composition of uRBCs and RBCs infected with asexual-stage parasites, male gametocytes or female gametocytes. In C, the three independent biological replicates are shown as points. In D, selected sphingolipid names are shown. Percentages for each principal component indicate the contribution of each component to overall variation between samples.

SMS1 and SMS2, which are expressed in a parasite stage- and sex-specific manner. SMS activity contributes to the synthesis of SM, a component of detergent-resistant lipid domains in cell membranes, but also catabolises the intracellular signalling molecule ceramide.

Three independent attempts to disrupt both SMS1 and SMS2 genes together did not yield any parasites after transfection. However, disruption of each SMS gene individually produced asexual blood-stage parasites that could be analysed further (Figs S1,S2). We first tested the relative fitness of these knockout (KO) parasites. In 28-day co-cultures, wild-type (WT) parasites quickly outgrew each of the KO parasites (Fig. 7), suggesting that SMS1 and SMS2 are each required for optimal asexual parasite proliferation. Depleting the culture medium lipids by 75% did not exacerbate the growth defect observed in each KO cell line (Fig. 7). In other words, SMS disruption is not readily compensated by an increase in extracellular lipid scavenging. Treatment with the sphingolipid synthesis inhibitor GT11 had the same effect on WT and each KO cell line (Fig. 7E). This suggests that GT11, an analogue of dihydroceramide, does not block SMS in asexual blood-stage parasites.

Given that sphingolipid composition is distinctive in gametocytes, the impact of disrupting each SMS was next investigated in sexual blood-stage parasites. The absence of either SMS1 or SMS2 increased gametocyte commitment compared to that of WT parasites (Fig. 7C,D). This may result from asexual blood-stage parasite stress, given that gametocyte commitment is a generic parasite stress response (Dixon et al., 2008). When treated with GT11, however, gametocytes lacking either SMS were hypersensitive compared to WT gametocytes (Fig. 7E). This suggests that SMS and dihydroceramide desaturase function is additive in gametocytes, especially in conditions where SMS function is limited either through disruption of one of the SMS genes (Fig. 7E) or by native reduction of SMS gene expression in males relative to females (Fig. 6).

DISCUSSION

In summary, the lipid composition and abundance of lipids in *P. falciparum* gametocytes is sex specific. Male–female gametocyte lipid dimorphism precedes gametocyte activation and reflects their sex-specific functions.

Female gametocyte-infected RBCs stockpile the neutral lipid CE (Fig. 8) but are resistant to the CE synthesis inhibitors Sandoz 58-035 and Glibenclamide. This suggests that acyl-coenzyme A: cholesterol acyltransferase-mediated CE synthesis is not essential in mature gametocytes. CE could instead be synthesised by

Journal of Cell Science (2022) 135, jcs259592. doi:10.1242/jcs.259592

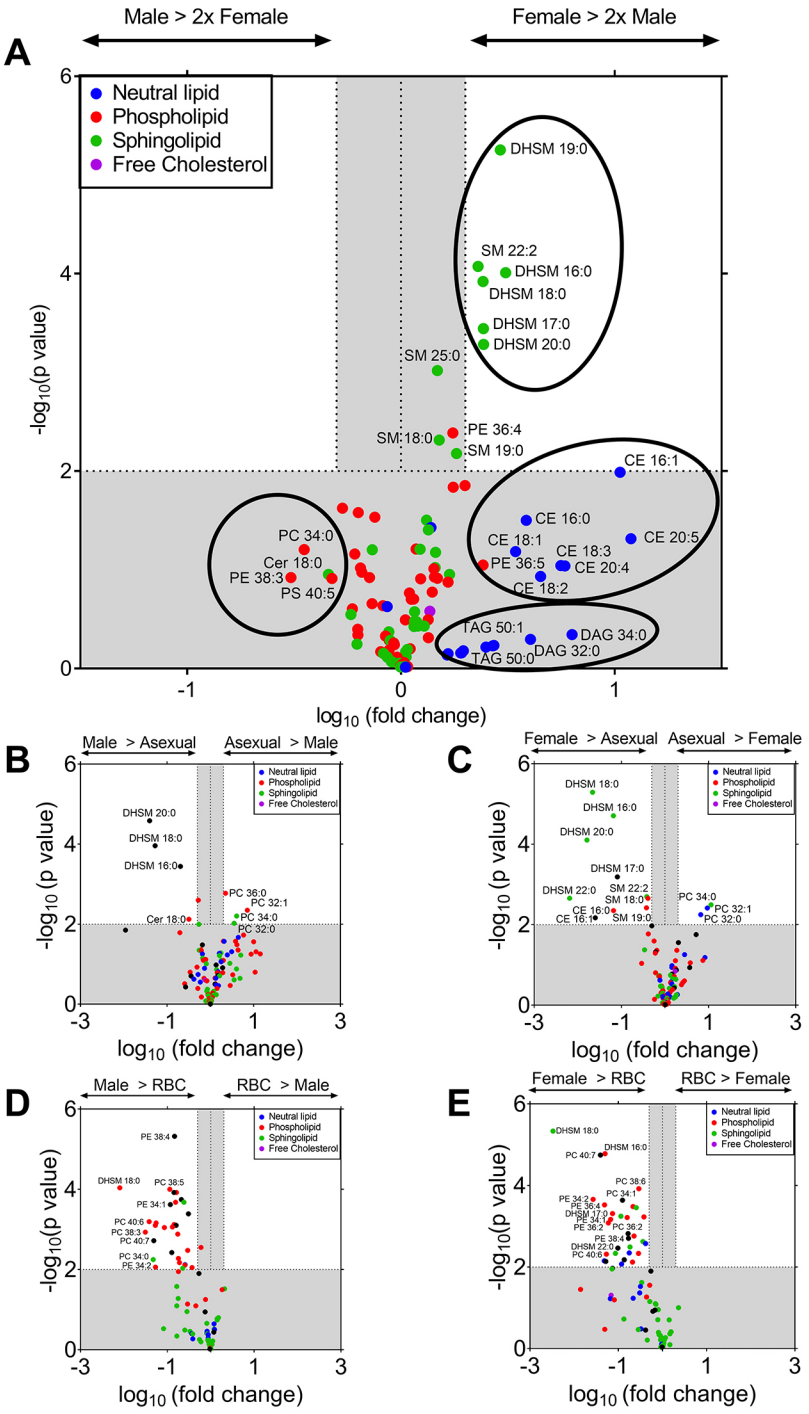

Fig. 5. Comparison of lipid species in male and female gametocyte-infected RBCs. (A,C,E) Comparison of female gametocyte-infected RBC lipids to male gametocyte-infected RBC lipids (A), asexual stage-infected RBC lipids (C) and uninfected RBC lipids (E). (B,D) Comparison of male gametocyte-infected RBC lipids to asexual stage-infected RBC lipids (B) and uninfected RBC lipids (D). Fold changes are averaged from three biological repeats of 10^7 cells each and are shown as $\log_{10}$ values. *P* values calculated using two-tailed paired Student's *t*-tests. Grey areas represent changes that are less than two-fold different between samples and/or have a significance of $P>0.01$. Circles in A highlight groups of lipids, and selected lipid names are shown.

lecithin–cholesterol acyltransferase or could be scavenged from the host. Alternatively, CE may only be required for later developmental stages. Indeed, the lipids in the fertilised zygote are exclusively contributed by the female gametocyte. While the zygote develops in the midgut lumen, neutral lipids are diverted from the blood meal to the eggs of the mosquito via lipophorin (Costa et al., 2018). The zygote is therefore vulnerable to lipid depletion in the mosquito midgut lumen and may depend on maternal CE reserves at this lifecycle stage. In particular, given that mosquitoes are incapable of cholesterol synthesis (Clayton, 1964), CE could be a source of cholesterol for the parasite during mosquito stages. *P. falciparum* encodes esterases that could potentially release cholesterol from CE stores (Butler et al., 2020). Neutral lipid staining of the female gametocyte has previously highlighted a large neutral lipid body in the cytoplasm (Tran et al., 2014). Potentially the female specific CE store is amassed by the putative lipid transporter gABCG2 (PlasmoDB: PF3D7_1426500). Hence, it would be interesting to test the effect of CE synthesis inhibitors on the mosquito stages in future studies.

Male gametocyte-infected RBCs do not contain more phospholipids than female gametocyte-infected RBCs (Fig. 8). Phospholipids are the main component of membranes and are likely required for the rapid cell divisions during male gametocyte activation when eight microgametes are formed within the male gametocyte. While additional plasma membranes may not be required in females, female gametocytes contain an elaborate

Journal of Cell Science (2022) 135, jcs259592. doi:10.1242/jcs.259592

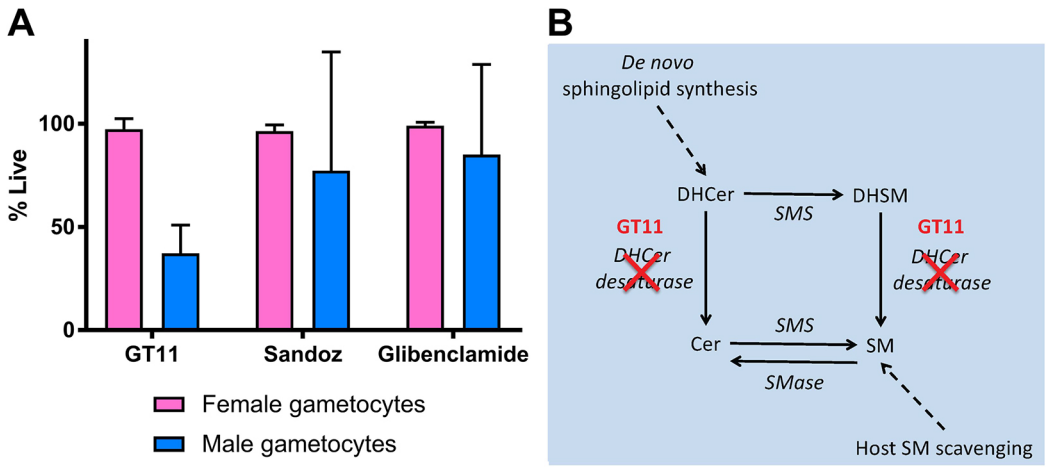

Fig. 6. Gametocyte viability following chemical inhibition of sphingolipid or CE synthesis. (A) Sphingolipid synthesis was disrupted with 10 µM GT11 and CE synthesis was inhibited with 10 µM Sandoz 58-035 or 10 µM glibenclamide from day 2 to day 6 post commitment. For each gametocyte sex, viability results are normalised to viability following exposure to the DMSO solvent control and 100 µM artemisinin (0% viable control). Data are presented as the mean±s.d. of three biological replicates, each performed in technical triplicates. (B) Diagram of GT11 inhibition of sphingolipid synthesis. Cer, ceramide; DHCer, dihydroceramide; SMase, sphingomyelinase.

mitochondrial network bound by a double membrane that is rich in phospholipids, as well as abundant membrane-bound osmiophilic bodies (Langreth et al., 1978; Jensen, 1979; Sinden, 1982; Ponnudurai et al., 1986). Although the total phospholipid content of male and female gametocyte-infected RBCs is similar, the allocation of phospholipids between organelles may be sex specific. For example, PG serves as the precursor for cardiolipin found exclusively in the mitochondria (Gebert et al., 2009; de Kroon et al., 1999; Daum, 1985). Consistent with this, PG is absent in uninfected RBCs, which lack mitochondria. Surprisingly, however, there is no difference in PG between male and female gametocytes despite female gametocytes relying more on their mitochondria than males. Indeed mitochondrial proteins have been shown to be more abundant in female gametocytes than in male gametocytes (Miao et al., 2017). Female gametes in the mosquito have an increased energy demand (probably in anticipation of the post-fertilisation stage; MacRae et al., 2013), whereas male gametocytes lose their mitochondria completely during the development into microgametes (Okamoto et al., 2009). The presence of comparable amounts of PG both in male and female gametocyte-infected RBCs argues for a similar number or size of mitochondria at least at the analysed stage of development (stage IV gametocytes). However, less PG is detected in RBCs infected with sexual stages compared to the RBCs infected with asexual stages, despite the upregulation of tricarboxylic acid cycle function in gametocytes (MacRae et al., 2013). This cautions against the simple correlation between PG and mitochondrial function. Nonetheless, the specificity and accumulation of PG in the parasite could be targeted by antimalarial compounds effective against both asexual and sexual blood-stage parasites.

Phospholipid composition distinguished both male and female gametocyte-infected RBCs from asexual parasite-infected RBCs and uninfected RBCs. Less phospholipids were present in gametocyte-infected RBCs compared to asexual parasite-infected RBCs, which is consistent with asexual replication requiring phospholipid-rich membrane biogenesis (for example, for the plasma membrane of a growing parasite, for merozoite formation and for RBC modifications such as Maurer's clefts). The increase in PS between trophozoites and gametocytes reported by Gulati et al. (2015) was not observed in this study, perhaps due to technical differences in sample preparation.

In asexual blood stages, reduction of sphingolipid metabolism by disruption of either SMS1 or SMS2 was not lethal but incurred a growth defect. Disruption of both SMS genes, on the other hand, appears to be lethal for asexual blood-stage parasites, despite SMS2 being expressed at very low levels in this lifecycle stage. This suggests that *de novo* SM synthesis is essential in asexual blood stages and indicates that each SMS is – to a certain degree – functionally redundant. Surprisingly, this defect was not exacerbated by depleting the culture medium lipids by 75%, or by inhibiting dihydroceramide desaturase using GT11. This supports the hypothesis that SMS activity regulates intracellular ceramide concentration rather than SM itself being essential for asexual blood-stage proliferation. Indeed, ceramide might otherwise build up to cytotoxic levels due to sphingomyelinase activity, which has previously been described in asexual stages (Hanada et al., 2002). Inhibition of ceramide production by sphingomyelinase with GW4869 is also lethal for asexual *P. falciparum* (Gulati et al., 2015), further illustrating the importance of regulating ceramide abundance.

The most distinctive feature of gametocyte-infected RBCs, particularly female gametocyte-infected RBCs, is the presence of DHSM species. This is consistent with other studies that suggest *de novo* sphingolipid synthesis, rather than host SM hydrolysis by neutral sphingomyelinase, is active in gametocytes (Gulati et al., 2015; Tran et al., 2016). Here, we sought to test whether DHSM accumulation in gametocytes results from decreased catabolism by dihydroceramide desaturase and/or from increased synthesis by SMS. Inhibition of dihydroceramide desaturase with 10 µM GT11 selectively killed male gametocytes (Fig. 6) suggesting that dihydroceramide desaturase activity is sex specific, which may contribute to the difference in DHSM abundance. The male-specific effect of GT11 was not observed in combined male and female gametocytes (Fig. 7E), presumably due to the gametocyte population being female biased. However, gametocytes that lack an SMS were hypersensitive to GT11 (Fig. 7E). In other words, reduced SMS activity (due to endogenous differential SMS gene expression between male and female gametocytes or through SMS

Journal of Cell Science (2022) 135, jcs259592. doi:10.1242/jcs.259592

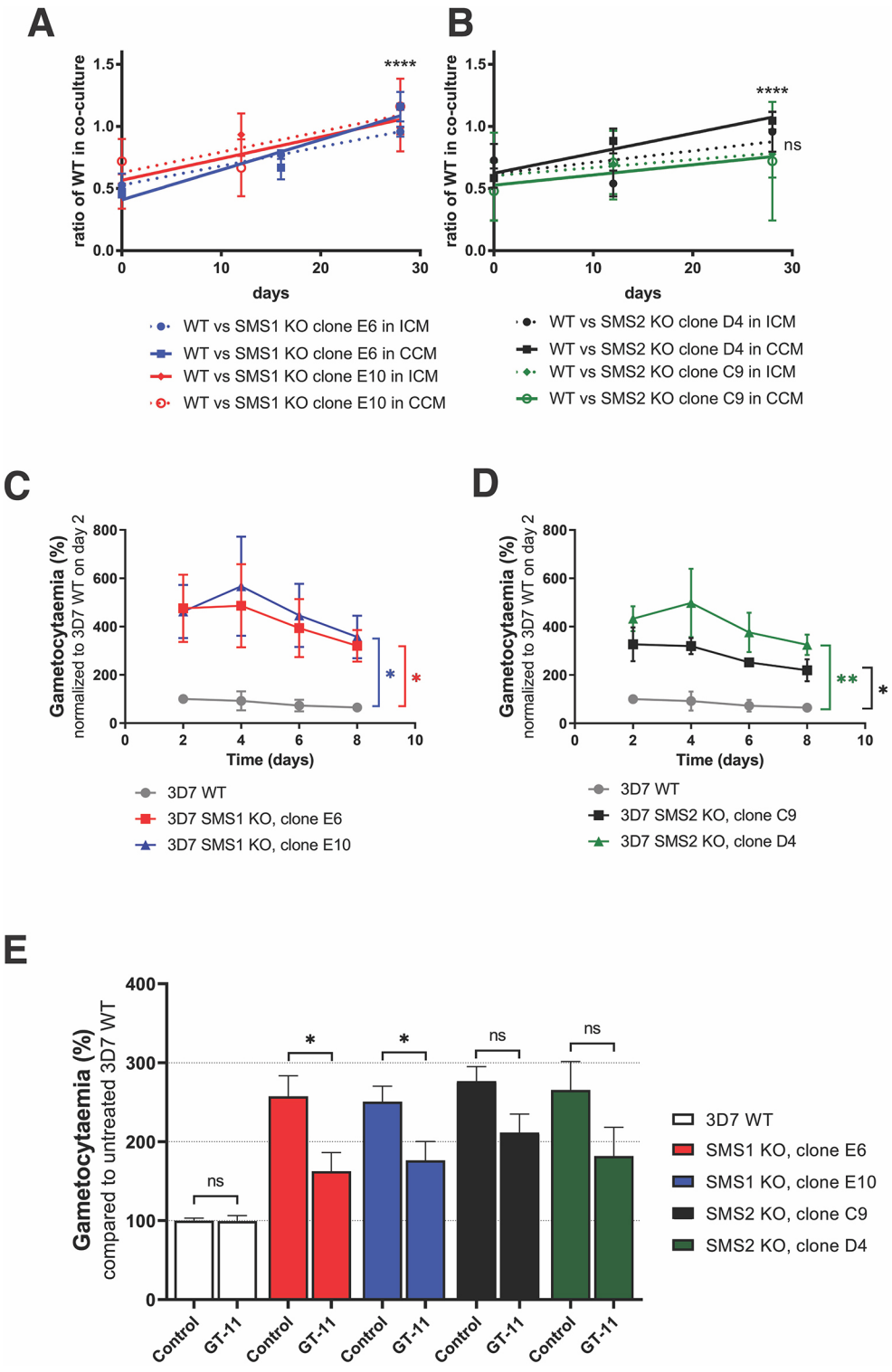

Fig. 7. Functional characterisation of SMS1 and SMS2 KO parasites. (A,B) Fitness competition at asexual intraerythrocytic stages between 3D7 WT and SMS1 KO (A) or SMS2 KO (B) clones in complete culture medium (CCM, continuous line) and lipid-depleted culture medium (ICM, dashed line) over 28 days. On day 0, equal amounts of 3D7 WT and SMS1 KO clone E6 (blue, A), SMS1 KO clone E10 (red, A), SMS2 KO clone C9 (green, B) or SMS2 KO clone D4 (black, B) were combined in a co-culture. The proportion of each genotype in the culture was monitored on day 0, 12 and 28 by qPCR of the hDHFR resistance cassette (to detect the KO genotype) and the disrupted section of the SMS1 or SMS2 genes (to detect the WT genotype). At some time points, technical problems inhibited monitoring the culture, so measurements were performed 4 days afterwards instead. Results from two to four independent biological repeats are shown as mean±s.d. Statistical significance between day 0 and day 28 was calculated by two-way ANOVA with Tukey's post hoc test. In B, results in ICM were not significant (ns), whereas $P<0.001$ for WT versus SMS1 clone E10 in ICM in A and ****$P<0.0001$ for all other results in A and B. (C,D) Gametocytaemia in 3D7 WT and SMS1 KO (C) or SMS2 KO clones (D) was monitored every second day from day 2 to day 8 post commitment and compared to WT gametocytaemia on day 2. (E) Effect of 10 µM GT11 on the commitment to gametocytaemia in 3D7 WT, SMS1 KO and SMS2 KO clones. The cultures were treated with GT11 (10 µM) or 0.1% DMSO (control) for 72 h from day 3 to day 0 pre-commitment. Gametocytaemia was determined on day 8 and compared to gametocytaemia of the untreated WT culture. In C–E, gametocytaemia is presented as mean±s.d. from three biological replicates, each performed in technical triplicates. *$P<0.05$; **$P<0.01$; ns, not significant, $P>0.1$ (two-tailed unpaired Student's *t*-test).

gene disruption) appears to make parasites more susceptible to dihydroceramide desaturase inhibition by GT11. Given that dihydroceramide desaturase and SMS share dihydroceramide as a substrate, hypersensitivity to GT11 in gametocytes with reduced SMS activity may result from an accumulation of dihydroceramide. Conversely, accumulation of DHSM in gametocytes may be a means of reducing intracellular dihydroceramide levels.

Similarly, the observed increased gametocyte commitment in SMS KO cell lines could be a stress response to elevated dihydroceramide concentrations. Indeed, it has recently been observed that dihydroceramides are biologically active lipids involved in diverse mammalian cell functions (Siddique et al., 2015). Lipids have previously been implicated in inducing gametocytogenesis in *P. falciparum* (Brancucci et al., 2017). In particular, depletion of serum lysophosphatidylcholine, a precursor of PC synthesis, is known to trigger gametocytogenesis. We observed no significant difference in lysophosphatidylcholine abundance between male and female gametocyte-infected RBCs (Fig. S3). PC is a substrate of

Journal of Cell Science (2022) 135, jcs259592. doi:10.1242/jcs.259592

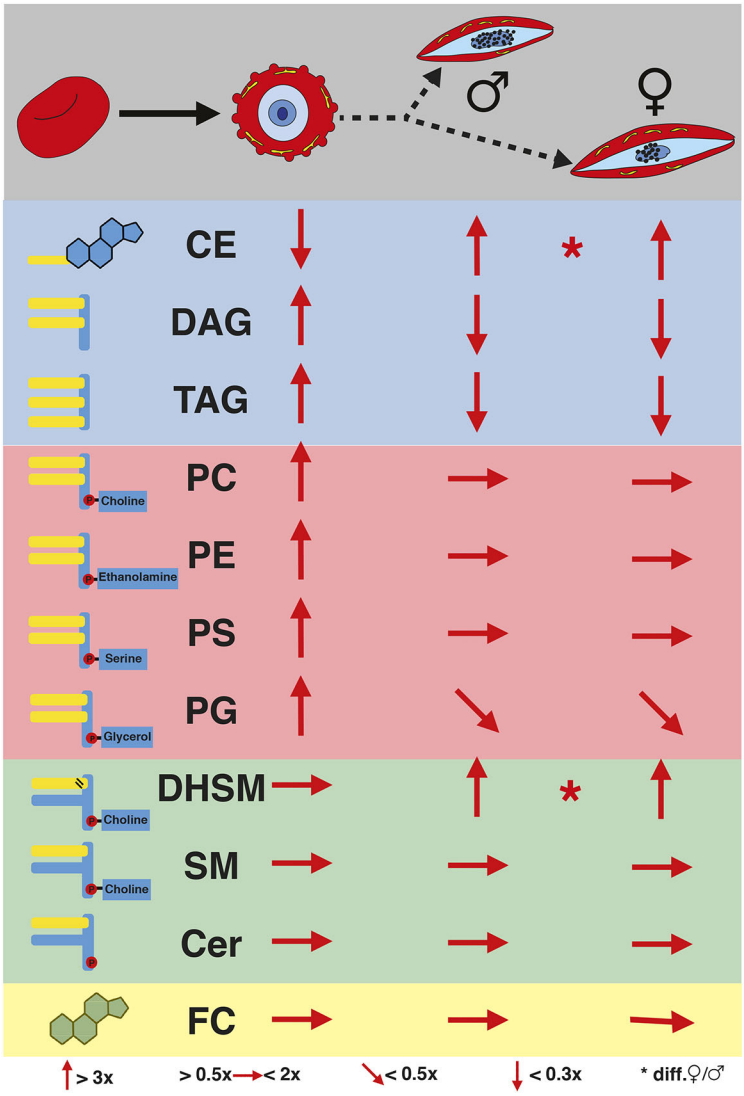

Fig. 8. Overview of lipid changes in *P. falciparum* during asexual and sexual blood stages. Grey background, left to right: graphic representation of uninfected RBCs, RBCs infected with trophozoite parasites, RBCs infected with male gametocytes and RBCs infected with female gametocytes. Dashed arrows indicate that there is no direct development from trophozoites to sexual stages, and the intermediate stages are not shown. Blue background, neutral lipids; red background, phospholipids; green background, sphingolipids; yellow background, free cholesterol. The left column shows graphic representations of the lipid groups and their abbreviations. The red arrows indicate changes relative to the previous life-cycle stage. Upward arrow means a greater than 3-fold increase; horizontal arrow means moderate or no changes (changes that are more than 0.5-fold and less than 2-fold); a declining arrow indicates decrease of less than 0.5-fold and a downward arrow signifies a decrease to less than 0.3× the previous value. Changes for RBCs infected with male and female gametocytes are relative to the trophozoite-infected RBCs. Asterisks indicate significant changes between RBCs infected with male or female gametocytes. Cer, ceramide.

SMS-mediated SM and DHSM synthesis. As such, reducing parasite SMS activity may have mimicked the downstream effect of PC depletion and triggered gametocytogenesis.

Overall, this study has shown that lipid metabolism is not only variable between parasite lifecycle stages but is also sex specific (Fig. 8). These differences have implications for the effectiveness of drugs targeting metabolic pathways and should be considered in the design of future transmission blocking antimalarial treatments. In terms of the fundamental biology of the parasite, the lipid profile of gametocytes is a testament to the parasite's ability to thrive in two radically different host environments. The lipidome presented here provides a reference for unravelling the complex sex-specific functions of lipids in *P. falciparum*.

MATERIALS AND METHODS

Culturing techniques

Asexual 3D7 strain *P. falciparum* parasites were maintained in complete culture medium [RPMI 1640-HEPES with Glutamax medium (Thermo Fisher Scientific) supplemented with 10 mM D-glucose, 480 µM hypoxanthine, 20 µg/ml gentamicin, 0.375% (w/v) Albumax II (Thermo Fisher Scientific) and 2.5% (v/v) heat-inactivated human serum (Australian Red Cross Lifeblood)] as previously described (Maier and Rug, 2013). Lipid-depleted culture medium consisted of complete culture medium without Albumax II. Human type O+ RBC and human serum donated from the Australian Red Cross Blood Bank were approved for experimental use by the Australian National University human ethics committee agreement 2017/351 and the Australian Red Cross agreement 17-06ACT-07. Cultures were synchronised by sorbitol treatment as described previously (Lambros and Vanderberg, 1979) and isolated from their host cells by saponin treatment (Dourmashkin et al., 1962).

Parasites were induced to form gametocytes as described previously by Fivelman et al. (2007) with modifications to reduce asexual parasite proliferation (Ridgway et al., 2020). Male and female gametocytes were collected by fluorescence-activated cell sorting (FACS) as described by Ridgway et al. (2021). Briefly, magnet-enriched 3D7 gametocytes with a female-specific GFP tag (gABCG2–GFP; Tran et al., 2014) were stained with Hoechst 33342 and collected by FACS on day 9 post commitment (mostly at stage IV). Hoechst staining identified gametocyte-infected from uninfected RBCs, while the female-specific GFP signal distinguished male and female gametocytes.

Gametocytaemia was measured every second day from day 2 post commitment by flow cytometry of an aliquot of culture stained with 50 µg/ml Hoechst 33342 in phosphate-buffered saline (PBS; 10.6 mM KH_2PO_4, 1.55 M NaCl, 29.7 mM Na_2HPO_4, pH 7.4) for 15 min at 37°C, rinsed twice in PBS with 2000 ***g***, 1 min centrifugations, and resuspended in PBS. Samples were analysed on a LSR II Flow Cytometer (BD Biosciences) detecting Hoechst 33342 in the Pacific Blue channel (350 nm excitation/461 nm emission). Parasitaemia was calculated as the proportion of Hoechst

33342-positive cells in 200,000 whole single cells as gated in FACS Diva software. Statistical significance and graphing of results was performed in GraphPad Prism 7.

Sex-specific gametocyte viability assay

Magnet-enriched gametocytes were exposed to 10 µM of each test compound, 200 µM artemisinin (0% viable control) or 0.1% (v/v) DMSO (100% viable control) for 96 h from day 2 to day 6 post commitment in complete culture medium with 50 mM N-acetyl D-glucosamine in a 96-well plate at 37°C in hypoxic conditions (1% O_2, 5% CO_2, 94% N_2).

Parasites were then stained in 50 µg/ml Hoechst 33342 and 500 nM MitoTracker Deep Red in complete culture medium supplemented with 50 mM N-acetyl D-glucosamine for 30 min at 37°C in hypoxic conditions (1% O_2, 5% CO_2, 94% N_2). Stained cells were rinsed twice in PBS with 1000 ***g***, 5 min centrifugations, and resuspended in PBS. Single-colour controls for flow cytometry consisted of (1) asexual 3D7 WT culture stained with 500 nM MitoTracker Deep Red or 50 µg/ml Hoechst 33342 for 30 min in complete culture medium, rinsed twice in PBS with 1000 ***g***, 1 min centrifugations, and resuspended in PBS; (2) unstained 3D7 gABCG2–GFP gametocytes suspended in PBS; and (3) unstained asexual 3D7 WT parasites in PBS (for the unstained control). Samples were analysed on a LSR II Flow Cytometer (BD Biosciences) detecting Hoechst 33342 in the Pacific Blue channel (405 nm excitation/461 nm emission), MitoTracker Deep Red in the APC-Cy7 channel (644 nm excitation/665 nm emission) and GFP in the FITC channel (488 nm excitation/509 nm emission). A total of 500,000 events were recorded in each single-colour control. In each sample, data was recorded until 500,000 female gametocytes were counted.

After applying the gating strategy to isolate male and female gametocytes (Ridgway et al., 2020), the mean fluorescence intensity of MitoTracker Deep Red detected on the APC-Cy7 channel was recorded for each of the gametocyte populations. Data was analysed in FlowJo, and statistical significance was determined by ANOVA with Sidak's multiple comparisons test in GraphPad Prism. Cell viability is expressed as a percentage of the mean fluorescence intensity of MitoTracker Deep Red in gametocytes treated with 0.1% DMSO (100% viable) and 200 µM artemisinin treated gametocytes (0% viable).

Generation of transgenic *P. falciparum* cell lines

The annotated sequence of *P. falciparum* 3D7 reference strain was sourced from the *Plasmodium* Genomics Resource PlasmoDB (www.plasmodb.org). To disrupt SMS1 (PF3D7_0625000) by double recombination, a 5′ fragment and a 3′ fragment of SMS1 locus were amplified using primers al398/al399 and al400/al401 (Table S1) and cloned into a pCC-1 vector containing a human dihydrofolate reductase (hDHFR) and 5-fluorocytosine drug selection cassette (Maier et al., 2008) at SacII/SpeI and EcoRI/AvrII sites to generate the pCC-1/SMS1 construct (Fig. S1). SMS2 (PF3D7_0625100) was also disrupted by double recombination by amplifying a 5′ fragment with al406/al407 primers and a 3′ fragment with al408/409 primers (Table S1), which were cloned into a pCC-1 vector at SacII/SpeI and EcoRI/AvrII sites to generate pCC-1/SMS2 construct (Fig. S2). Given that SMS1 and SMS2 are adjacent genes, a pCC-1/SMS1 and 2 construct aiming to disrupt both SMS genes was generated by cloning the 5′ fragment of SMS1 (amplified with al398/al399 primers) and the 3′ fragment of SMS2 (amplified with al408/al409 primers) at SacII/SpeI and EcoRI/AvrII sites. Inserted DNA regions were confirmed by analytical restriction enzyme digest and were sequenced to verify constructs. Plasmids were purified using Invitrogen Purelink Maxiprep kit prior to transfection.

P. falciparum 3D7 reference strain parasites were transfected as described previously (Rug and Maier, 2013). Briefly, 400 µl of 100 µg plasmid DNA in Cytomix [120 mM KCl, 0.15 mM $CaCl_2$, 10 mM K_2HPO_4/KH_2PO_4, 25 mM HEPES, 2 mM ethylene glycol-bis(β-aminoethyl ether)-tetraacetic acid, 5 mM $MgCl_2$, pH 7.6] was electroporated into a sorbitol-synchronised ring-stage culture at 5% parasitaemia by 310V, 950 µF pulse delivered in a 0.2 cm electrode gap cuvette placed in a Bio-Rad Genepulser II with ∞ capacitor. Transformed cells were immediately resuspended in complete culture medium with 3% haematocrit uninfected RBCs and incubated at 37°C in hypoxic conditions (1% O_2, 5% CO_2, 94% N_2). Culture medium was supplemented with 2 nM WR99210 from 4 h post transfection and was replaced daily for 5 days post transfection, then three times a week until parasites were observed by Giemsa-stained thin smears of the culture. Parasites having integrated the plasmid were enriched by three 21-day off/on 2 nM WR99210 cycles, then negative selection was applied by adding 231 nM 5-fluorocytosine. The transgenic parasites were cloned by limited dilution (Rug and Maier, 2013).

DNA extraction

Genomic DNA was extracted from saponin-isolated trophozoite-stage parasites using DNeasy Blood and Tissue kit (Qiagen) as per the manufacturer's instructions. For Southern blot analysis, genomic DNA was eluted twice in 200 µl elution buffer each then concentrated by adding 40 µl 3 M sodium acetate and 880 µl 100% ethanol at 4°C overnight. Samples were centrifuged at 17,000 ***g*** for 30 min at 4°C, then DNA was washed twice in 70% ethanol with 17,000 ***g***, 20 min centrifugations. DNA was air dried then resuspended in TE buffer (10 mM Tris-base, 1 mM EDTA, pH 8.0). DNA concentration and purity were measured using a NanoDrop spectrophotometer (Thermo Fisher Scientific).

Quantitative PCR

The abundance of WT and KO genotypes in co-cultures was monitored by quantitative PCR (qPCR) of regions of DNA specific to each genome. SMS1 KO and SMS2 KO parasites were each quantified by primers specific to the sequence of the inserted hDHFR drug resistance cassette. WT parasites were distinguished from SMS1 KO parasites by primers specific to the region of SMS1 disrupted by homologous recombination in the SMS1 KO parasites. WT parasites in the SMS2 KO/WT co-cultures were similarly quantified by primers specific to the disrupted section of SMS2 in the SMS2 KO parasites. The primers for this experiment are described in Table S2.

qPCR was performed using a Light Cycler 480 SYBR Green I Master mix (Roche) as per the manufacturer's instructions for 10 µl reactions in a 384-well plate. Thermocycling was performed with a 10 min, 95°C pre-incubation; 45 cycles of 15 s denaturation at 95°C, 15 s annealing at 52°C and 20 s elongation at 72°C; followed by a melt curve established by denaturing at 95°C for 30 s, annealing at 60°C for 30 s and then slowly denaturing by increasing the temperature to 95°C at 0.11°C/s. Melt curves were observed using Light Cycler 480 software. The exported text file was converted using Light Cycler 480 converter (Roche), and Cq and PCR efficiencies were determined using the LinReg program (Ruijter et al., 2009). Relative quantification of transcripts was expressed as described previously (Pfaffl, 2001).

For the quantification of WT and KO parasite genotypes in co-cultures we calculated the following ratio:

$$\text{ratio}=[E_{\text{target}}^{\Delta CP\text{target(clonal}-\text{competition)}}]/[E_{\text{ref}}^{\Delta CP\text{ref(clonal}-\text{competition)}}],$$

where E_{target} is the primer efficiency of the target gene; E_{ref} is the primer efficiency of the reference gene; $\Delta CP\text{target}^{(\text{clonal}-\text{competition})}$ is the difference in crossing points of target gene amplification in a clonal population and the fitness competition co-culture; and $\Delta CP\text{ref}^{(\text{clonal}-\text{competition})}$ is the difference in crossing points of reference gene amplification in a clonal population and the fitness competition co-culture.

Southern blotting

Disruption of a gene locus by homologous recombination was confirmed by diagnostic digest with restriction enzymes followed by Southern blots probing for both the 5′ and 3′ homologous regions (Rug and Maier, 2013). DNA was digested with either AflII and PacI (for SMS1 KO screening) or Xmn I and Hind III-HF (for SMS2 KO screening), as per the manufacturer's instructions, then run on a 0.8% agarose gel at 90V for 15 min followed by a run at 20V for 18 h. The gel was then rinsed as follows: 15 min in depurination solution (0.25 M HCl); 3 min in milliQ water; 2×15 min in denaturation solution (0.5 M NaOH, 1.5 M NaCl); 3 min in milliQ water; 2×15 min in neutralisation solution (0.5 M Tris-base, 1.5 M NaCl, pH 7.5);

3 min in milliQ water then 5 min in 20× SCC (3 M NaCl, 0.3 M citric acid trisodium dihydrate, pH 7.0). DNA was transferred from the gel to the membrane overnight in a capillary transfer setup.

Alkali-labile digoxigenin-labelled deoxyuridine triphosphate (DIG–dUTP) was incorporated in Southern blot probes by PCR using a PCR DIG Probe Synthesis kit (Roche) with the following specifications (refer to sequences in Table S3). Each probe was amplified from the corresponding plasmid using either OneTaq (NEB) or Taq polymerase (Roche). SMS1 probes were purified by gel extraction (Qiagen kit). All probes were synthesised in the presence of 12 µM DIG–dUTP except the SMS2 3′ probe, which was synthesised from 6 µM DIG-dUTP. Thermocycling conditions consisted of initial denaturation for 30 s at 94°C; 30 cycles of 30 s at 94°C, 1 min at 45°C (SMS2 3′) or 50°C (SMS2 5′) or 52°C (SMS1 5′) or 55°C (SMS1 3′), 1 min at 68°C; final elongation for 7 min at 68°C.

Following transfer, the membrane was rinsed in 2× SCC for 5 min, then DNA was crosslinked to the membrane in a UV crosslinker set to deliver 70 mJ/cm^2. The membrane was incubated with gentle rocking in DIG Easy Hyb solution (Roche, 11 796 895 001) at the respective probe hybridisation temperature (T_{hyb}) for 30 min. The probe was denatured in 50 µl water at 95°C for 5 min, cooled quickly on ice then added to DIG Easy Hyb solution at 0.15% (v/v) to prepare the hybridisation solution. The membrane was incubated overnight in hybridisation solution at T_{hyb} with gentle rocking.

The membrane was prepared for detection by rinsing in 2× SCC for 5 min; equilibrating in washing buffer for 1 min [0.1 M maleic acid, 0.15 M NaCl, pH 7.5 with 0.3% (v/v) Tween-20]; incubating in 1% blocking solution [0.1 M maleic acid, 0.15 M NaCl, pH 7.5 with 1% (w/v) skim milk powder] for 30 min; incubating in 1% blocking solution with 1:10,000 α-Digoxigenin-AP Fab fragments (Roche) for 30 min; washing membrane in washing buffer for 2×15 min then equilibrating membrane in detection buffer (100 mM Tris-HCl, 100 mM NaCl, pH 9.5) for 2 min. The membrane was incubated in the dark with CSPD (Roche) diluted 1:100 in detection buffer for 5 min at room temperature then 10 min at 37°C. The membrane was exposed to Fuji Super RX-N Medical X-Ray film in an Amersham Pharmacia Biotech hypercassette, and film was developed in an AGFA CP1000 photo developer.

Lipidomic analysis

Uninfected human RBCs from six donors (Australian Red Cross) were pooled in three independent biological replicates each from two donors and incubated at 4% haematocrit in complete culture medium for at least 48 h at 37°C in hypoxic conditions (1% O_2, 5% CO_2, 94% N_2). Cells were pelleted at 524 ***g*** over 5 min and counted on an Improved Neubauer haemocytometer (Hirschmann). Aliquots of 10^7 cells were resuspended in 300 µl of methanol in 2 ml tough tubes (Geneworks) and stored at −80°C. For each biological replicate, parasites of different stages were grown in the same donor batch of RBCs to reduce host-specific influences.

For collection of asexual parasite-infected RBCs, three independent asexual *P. falciparum* cultures were sorbitol synchronised then magnet purified to more than 98% iRBCs, as determined by Giemsa-stained thin smear, and counted on an Improved Neubauer haemocytometer (Hirschmann). Aliquots of 10^7 iRBCs at 26–42 h post invasion were resuspended in 300 µl of methanol in 2 ml tough tubes (Geneworks) and stored at −80°C.

Male and female gametocytes were sorted live by FACS as described above, pelleted at 754 ***g*** for 10 min and resuspended in 300 µl of methanol per 10^7 cells (as counted during FACS) in 2 ml tough tubes (Geneworks). Each biological replicate of 10^7 cells was pooled from 2–5 independent gametocyte cultures.

Lipids were extracted as described previously (Matyash et al., 2008) with modifications. Internal standards (Tran et al., 2016) in 50 µl of methanol with 0.01% butylated hydroxytoluene were aliquoted among tubes. Internal standards and 1.4 mm beads (Geneworks) were added to tough tubes containing samples in 300 µl methanol, and samples were homogenised with a bead homogeniser (FastPrep-24, MP Biomedical) at 6 m/s for 40 s and transferred to new tubes. Beads were rinsed in 100 µl of methanol, which was added to the sample in new tubes. Samples were vortexed with 1 ml of methyl tert-butyl ether at 4°C for 1 h. Phase separation was induced by adding 300 µl of 150 mM ammonium acetate (liquid chromatography–MS grade, Fluka), vortexing for 5 min and centrifuging at 2000 ***g*** for 5 min. The upper organic layer (representing around 800 µl) was transferred to a 2 ml glass vial and stored at −20°C. Prior to mass spectrometry analysis, each sample was diluted into methanol:chloroform (2:1 v/v) with 5 mM ammonium acetate.

An aliquot of each extract was hydrolysed to remove acyl-linked lipids and re-extracted to improve mass spectrometric analysis of sphingolipids. A 200 µl volume of extract was added to 60 µl of methanol containing 0.01% butylated hydroxytoluene, 22 µl of 10 M NaOH was added (final concentration 0.7 M), and the sample was vortexed at 800 rounds per minute on an Eppendorf Mixmate for 2 h at room temperature. A 60 µl volume of 150 mM aqueous ammonium acetate was added to induce phase separation. Tubes were vortexed and spun at 20,000 ***g*** for 5 min to complete phase separation. The upper organic layer was removed to a new 2 ml glass vial and diluted into methanol:chloroform (2:1 v/v) containing 5 mM ammonium acetate prior to mass spectrometric analysis.

Mass spectra were obtained with a chip-based nanoESI source (TriVersa Nanomate, Advion) and a hybrid linear ion-trap-triple quadrupole mass spectrometer (QTRAP 5500, ABSCIEX). A 10 µl volume of each sample extract in a sealed Eppendorf Twin-Tec 96-well plate was aspirated and delivered to the mass spectrometer through a nanoESI chip. Positive ion and negative ion acquisition was obtained as described previously (Tran et al., 2016).

Data smoothing, lipid identification, removal of isotope contribution from lower mass species and correction for isotope distribution was performed in LipidView (ABSCIEX) software version 1.2. A signal to noise ratio threshold of 20 was applied for inclusion of ionised lipids. Extraction and solvent blanks were analysed in each data acquisition batch to exclude chemical or solvent impurities. Lipids were quantified in LipidView by comparing peak area of each lipid to its class-specific internal standard after isotope correction. Where odd-chain fatty acid phospholipids or ether-linked phospholipids could not be distinguished, phospholipids were assumed to be ether linked. A correction factor of 3.45 was applied to all ether-PE species to account for the ∼29% difference in efficiency in the neutral loss of the 141 Da fragment from plasmenyl and diacyl PE, respectively (Mitchell et al., 2007; Abbott et al., 2013). Lipid species are annotated as per Liebisch et al. (2013) shorthand, except for DAG and TAG.

LipidView data was exported to Microsoft Excel then imported to Markerview v1.2.1.1 (Applied Biosystems, MDS Sciex) with lipid annotation and quantification for statistical analysis of all individual lipid species. Pareto scaling without weighting was applied for unsupervised mode principal component analysis. Multiple *t*-tests for volcano plots were also performed in MarkerView (MDS Sciex). Grouping into lipid classes and calculation of lipid proportions were performed in Microsoft Excel. GraphPad Prism 7 was used to prepare graphs and perform ANOVA with Tukey's multiple comparison test on lipid class abundance.

Acknowledgements

FACS was performed with assistance from Dr Harpeet Vohra and Mr Michael Devoy. We are grateful to the Australian Red Cross for providing human red blood cells and serum.

Competing interests

The authors declare no competing or financial interests.

Author contributions

Conceptualization: M.C.R., A.G.M.; Methodology: M.C.R., D.C., S.H.J.B., T.W.M., A.G.M.; Validation: M.C.R.; Formal analysis: M.C.R., D.C., S.H.J.B., T.W.M., A.G.M.; Investigation: M.C.R., D.C., S.H.J.B., P.T.; Data curation: S.H.J.B.; Writing - original draft: M.C.R., A.G.M.; Writing - review & editing: M.C.R., D.C., S.H.J.B., P.T., T.W.M., A.G.M.; Visualization: M.C.R., D.C., A.G.M.; Supervision: A.G.M.; Project administration: A.G.M.; Funding acquisition: A.G.M.

Funding

Funding was provided by the Australian Research Council (DP180103212) and the National Health and Medical Research Council of Australia (APP1182369). M.C.R. is supported by the Australian Government Research Training Program Scholarship and The Australian National University.

Data availability

The raw mass spectrometry data from the lipidomics experiments have been deposited in the MetaboLights database with accession number MTBLS4137.

References

Abbott, S. K., Jenner, A. M., Mitchell, T. W., Brown, S. H. J., Halliday, G. M. and Garner, B. (2013). An improved high-throughput lipid extraction method for the analysis of human brain lipids. *Lipids* **48**, 307-318. doi:10.1007/s11745-013-3760-z

Aikawa, M., Carter, R., Ito, Y. and Nijhout, M. (1984). New observations on gametogenesis, fertilization, and zygote transformation in *Plasmodium gallinaceum*. *J. Protozool.* **31**, 403-413. doi:10.1111/j.1550-7408.1984.tb02987.x

Bedia, C., Triola, G., Casas, J., Llebaria, A. and Fabriàs, G. (2005). Analogs of the dihydroceramide desaturase inhibitor GT11 modified at the amide function: synthesis and biological activities. *Org. Biomol. Chem.* **3**, 3707-3712. doi:10.1039/b510198k

Bennink, S., Kiesow, M. J. and Pradel, G. (2016). The development of malaria parasites in the mosquito midgut. *Cell. Microbiol.* **18**, 905-918. doi:10.1111/cmi.12604

Brancucci, N. M. B., Gerdt, J. P., Wang, C. Q., De Niz, M., Philip, N., Adapa, S. R., Zhang, M., Hitz, E., Niederwieser, I., Boltryk, S. D. et al. (2017). Lysophosphatidylcholine regulates sexual stage differentiation in the human malaria parasite *Plasmodium falciparum*. *Cell* **171**, 1532-1544.e15. doi:10.1016/j.cell.2017.10.020

Butler, J. H., Baptista, R. P., Valenciano, A. L., Zhou, B., Kissinger, J. C., Tumwebaze, P. K., Rosenthal, P. J., Cooper, R. A., Yue, J.-M. and Cassera, M. B. (2020). Resistance to some but not other dimeric lindenane sesquiterpenoid esters is mediated by mutations in a *Plasmodium falciparum* esterase. *ACS Infectious Diseases* **6**, 2994-3003. doi:10.1021/acsinfecdis.0c00487

Canning, E. U. and Sinden, R. E. (1975). Nuclear organisation in gametocytes of *Plasmodium* and Hepatocystis: a cytochemical study. *Z. Parasitenkund.* **46**, 297-299. doi:10.1007/BF00418523

Clayton, R. B. (1964). The utilization of sterols by insects. *J. Lipid Res.* **5**, 3-19. doi:10.1016/S0022-2275(20)40254-8

Costa, G., Gildenhard, M., Eldering, M., Lindquist, R. L., Hauser, A. E., Sauerwein, R., Goosmann, C., Brinkmann, V., Carrillo-Bustamante, P. and Levashina, E. A. (2018). Non-competitive resource exploitation within mosquito shapes within-host malaria infectivity and virulence. *Nat. Commun.* **9**, 3474. doi:10.1038/s41467-018-05893-z

Daum, G. (1985). Lipids of mitochondria. *Biochim. Biophys. Acta* **822**, 1-42. doi:10.1016/0304-4157(85)90002-4

de Kroon, A. I. P. M., Koorengevel, M. C., Goerdayal, S. S., Mulders, P. C., Janssen, M. J. and de Kruijff, B. (1999). Isolation and characterization of highly purified mitochondrial outer membranes of the yeast *Saccharomyces cerevisiae* (method). *Mol. Membr. Biol.* **16**, 205-211. doi:10.1080/096876899294670

Dixon, M. W. A., Thompson, J., Gardiner, D. L. and Trenholme, K. R. (2008). Sex in *Plasmodium*: a sign of commitment. *Trends Parasitol.* **24**, 168-175. doi:10.1016/j.pt.2008.01.004

Dourmashkin, R. R., Dougherty, R. M. and Harris, R. J. (1962). Electron microscopic observations on Rous sarcoma virus and cell membranes. *Nature* **194**, 1116-1119. doi:10.1038/1941116a0

Fivelman, Q. L., Mcrobert, L., Sharp, S., Taylor, C. J., Saeed, M., Swales, C. A., Sutherland, C. J. and Baker, D. A. (2007). Improved synchronous production of *Plasmodium falciparum* gametocytes *in vitro*. *Mol. Biochem. Parasitol.* **154**, 119-123. doi:10.1016/j.molbiopara.2007.04.008

Fyrst, H. and Saba, J. D. (2010). An update on sphingosine-1-phosphate and other sphingolipid mediators. *Nat. Chem. Biol.* **6**, 489-497. doi:10.1038/nchembio.392

Gardner, M. J., Hall, N., Fung, E., White, O., Berriman, M., Hyman, R. W., Carlton, J. M., Pain, A., Nelson, K. E., Bowman, S. et al. (2002). Genome sequence of the human malaria parasite *Plasmodium falciparum*. *Nature* **419**, 498-511. doi:10.1038/nature01097

Gebert, N., Joshi, A. S., Kutik, S., Becker, T., Mckenzie, M., Guan, X. L., Mooga, V. P., Stroud, D. A., Kulkarni, G., Wenk, M. R. et al. (2009). Mitochondrial cardiolipin involved in outer-membrane protein biogenesis: implications for Barth syndrome. *Curr. Biol.* **19**, 2133-2139. doi:10.1016/j.cub.2009.10.074

Gulati, S., Ekland, E. H., Ruggles, K. V., Chan, R. B., Jayabalasingham, B., Zhou, B., Mantel, P.-Y., Lee, M. C. S., Spottiswoode, N., Coburn-Flynn, O. et al. (2015). Profiling the essential nature of lipid metabolism in asexual blood and gametocyte stages of *Plasmodium falciparum*. *Cell Host Microbe* **18**, 371-381. doi:10.1016/j.chom.2015.08.003

Hanada, K., Palacpac, N. M. Q., Magistrado, P. A., Kurokawa, K., Rai, G., Sakata, D., Hara, T., Horii, T., Nishijima, M. and Mitamura, T. (2002). *Plasmodium falciparum* phospholipase C hydrolyzing sphingomyelin and lysocholinephospholipids is a possible target for malaria chemotherapy. *J. Exp. Med.* **195**, 23-34. doi:10.1084/jem.20010724

Jensen, J. B. (1979). Observations on gametogenesis in *Plasmodium falciparum* from continuous culture. *J. Protozool.* **26**, 129-132. doi:10.1111/j.1550-7408.1979.tb02748.x

Lambros, C. and Vanderberg, J. P. (1979). Synchronization of *Plasmodium falciparum* erythrocytic stages in culture. *J. Parasitol.* **65**, 418-420. doi:10.2307/3280287

Langreth, S. G., Jensen, J. B., Reese, R. T. and Trager, W. (1978). Fine structure of human malaria *in vitro*. *J. Protozool.* **25**, 443-452. doi:10.1111/j.1550-7408.1978.tb04167.x

Lasonder, E., Rijpma, S. R., Van Schaijk, B. C. L., Hoeijmakers, W. A. M., Kensche, P. R., Gresnigt, M. S., Italiaander, A., Vos, M. W., Woestenenk, R., Bousema, T. et al. (2016). Integrated transcriptomic and proteomic analyses of *P. falciparum* gametocytes: molecular insight into sex-specific processes and translational repression. *Nucleic Acids Res.* **44**, 6087-6101. doi:10.1093/nar/gkw536

Liebisch, G., Vizcaíno, J. A., Köfeler, H., Trötzmüller, M., Griffiths, W. J., Schmitz, G., Spener, F. and Wakelam, M. J. O. (2013). Shorthand notation for lipid structures derived from mass spectrometry. *J. Lipid Res.* **54**, 1523-1530. doi:10.1194/jlr.M033506

López-Barragán, M. J., Lemieux, J., Quiñones, M., Williamson, K. C., Molina-Cruz, A., Cui, K., Barillas-Mury, C., Zhao, K. and Su, X.-z. (2011). Directional gene expression and antisense transcripts in sexual and asexual stages of *Plasmodium falciparum*. *BMC Genomics* **12**, 587. doi:10.1186/1471-2164-12-587

MacRae, J. I., Dixon, M. W. A., Dearnley, M. K., Chua, H. H., Chambers, J. M., Kenny, S., Bottova, I., Tilley, L. and Mcconville, M. J. (2013). Mitochondrial metabolism of sexual and asexual blood stages of the malaria parasite *Plasmodium falciparum*. *BMC Biol.* **11**, 67. doi:10.1186/1741-7007-11-67

Maier, A. G. and Rug, M. (2013). In vitro culturing Plasmodium falciparum erythrocytic stages. *Method. Mol. Biol.* **923**, 3-15. doi:10.1007/978-1-62703-026-7_1

Maier, A. G., Rug, M., O'neill, M. T., Brown, M., Chakravorty, S., Szestak, T., Chesson, J., Wu, Y., Hughes, K., Coppel, R. L. et al. (2008). Exported proteins required for virulence and rigidity of *Plasmodium falciparum*-infected human erythrocytes. *Cell* **134**, 48-61. doi:10.1016/j.cell.2008.04.051

Matyash, V., Liebisch, G., Kurzchalia, T. V., Shevchenko, A. and Schwudke, D. (2008). Lipid extraction by methyl-tert-butyl ether for high-throughput lipidomics. *J. Lipid Res.* **49**, 1137-1146. doi:10.1194/jlr.D700041-JLR200

Miao, J., Chen, Z., Wang, Z., Shrestha, S., Li, X., Li, R. and Cui, L. (2017). Sex-specific biology of the human malaria parasite revealed from the proteomes of mature male and female gametocytes. *Mol. Cell. Proteomics* **116**, 061804. doi:10.1074/mcp.M116.061804

Mitchell, T. W., Buffenstein, R. and Hulbert, A. J. (2007). Membrane phospholipid composition may contribute to exceptional longevity of the naked mole-rat (*Heterocephalus glaber*): a comparative study using shotgun lipidomics. *Exp. Gerontol.* **42**, 1053-1062. doi:10.1016/j.exger.2007.09.004

Okamoto, N., Spurck, T. P., Goodman, C. D. and Mcfadden, G. I. (2009). Apicoplast and mitochondrion in gametocytogenesis of *Plasmodium falciparum*. *Eukaryot. Cell* **8**, 128-132. doi:10.1128/EC.00267-08

Pfaffl, M. W. (2001). A new mathematical model for relative quantification in real-time RT-PCR. *Nucleic Acids Res.* **29**, e45. doi:10.1093/nar/29.9.e45

Ponnudurai, T., Lensen, A. H. W., Meis, J. F. G. M. and Meuwissen, J. H. E. T. (1986). Synchronization of *Plasmodium falciparum* gametocytes using an automated suspension culture system. *Parasitology* **93**, 263-274. doi:10.1017/S003118200005143X

Ridgway, M. C., Shea, K. S., Cihalova, D. and Maier, A. G. (2020). Novel method for the separation of male and female gametocytes of the malaria parasite *Plasmodium falciparum* that enables biological and drug discovery. *mSphere* **5**, e00671-20. doi:10.1128/mSphere.00671-20

Ridgway, M. C., Cihalova, D. and Maier, A. G. (2021). Sex-specific separation of *Plasmodium falciparum* gametocyte populations. *Bio-protocol* **11**, e4045. doi:10.21769/BioProtoc.4045

Ross, A. C., Go, K. J., Heider, J. G. and Rothblat, G. H. (1984). Selective inhibition of acyl coenzyme A:cholesterol acyltransferase by compound 58-035. *J. Biol. Chem.* **259**, 815-819. doi:10.1016/S0021-9258(17)43530-7

Rug, M. and Maier, A. G. (2013). Transfection of *Plasmodium falciparum*. *Method. Mol. Biol.* **923**, 75-98. doi:10.1007/978-1-62703-026-7_6

Ruijter, J. M., Ramakers, C., Hoogaars, W. M. H., Karlen, Y., Bakker, O., Van Den Hoff, M. J. B. and Moorman, A. F. M. (2009). Amplification efficiency: linking baseline and bias in the analysis of quantitative PCR data. *Nucleic Acids Res.* **37**, e45. doi:10.1093/nar/gkp045

Siddique, M. M., Li, Y., Chaurasia, B., Kaddai, V. A. and Summers, S. A. (2015). Dihydroceramides: from bit players to lead actors. *J. Biol. Chem.* **290**, 15371-15379. doi:10.1074/jbc.R115.653204

Sinden, R. E. (1982). Gametocytogenesis of *Plasmodium falciparum in vitro*: an electron microscopic study. *Parasitology* **84**, 1-11. doi:10.1017/S003118200005160X

Sinden, R. E., Hartley, R. H. and Winger, L. (1985). The development of *Plasmodium* ookinetes *in vitro*: an ultrastructural study including a description of meiotic division. *Parasitology* **91**, 227-244. doi:10.1017/S0031182000057334

Sinden, R. E., Brown, S. H. J., Mitchell, T. W., Matuschewski, K., Mcmillan, P. J., Kirk, K., Dixon, M. W. A. and Maier, A. G. (1978). Gametocyte and gamete development in Plasmodium falciparum. *Proc. R. Soc. Lond. B Biol. Sci.* **201**, 375-399. doi:10.1098/rspb.1978.0051

Tran, P. N.,, Brown, S. H. J., Mitchell, T. W., Matuschewski, K., McMillan, P. J., Kirk, K., Dixon, M. W. A. and Maier, A. G. (2014). A female gametocyte-specific ABC transporter plays a role in lipid metabolism in the malaria parasite. *Nat. Commun.* **5**, 4773. doi:10.1038/ncomms5773

Tran, P. N., Brown, S. H. J., Rug, M., Ridgway, M. C., Mitchell, T. W. and Maier, A. G. (2016). Changes in lipid composition during sexual development of the malaria parasite *Plasmodium falciparum*. *Malar. J.* **15**, 73. doi:10.1186/s12936-016-1130-z

Triola, G., Fabrias, G., Dragusin, M., Niederhausen, L., Broere, R., Llebaria, A. and Van Echten-Deckert, G. (2004). Specificity of the dihydroceramide desaturase inhibitor N-[(1R,2S)-2-hydroxy-1-hydroxymethyl-2-(2-tridecyl-1-cyclopropenyl)ethyl]octanamide (GT11) in primary cultured cerebellar neurons. *Mol. Pharmacol.* **66**, 1671-1678. doi:10.1124/mol.104.003681

Vlachou, D., Zimmermann, T., Cantera, R., Janse, C. J., Waters, A. P. and Kafatos, F. C. (2004). Real-time, *in vivo* analysis of malaria ookinete locomotion and mosquito midgut invasion. *Cell. Microbiol.* **6**, 671-685. doi:10.1111/j.1462-5822.2004.00394.x

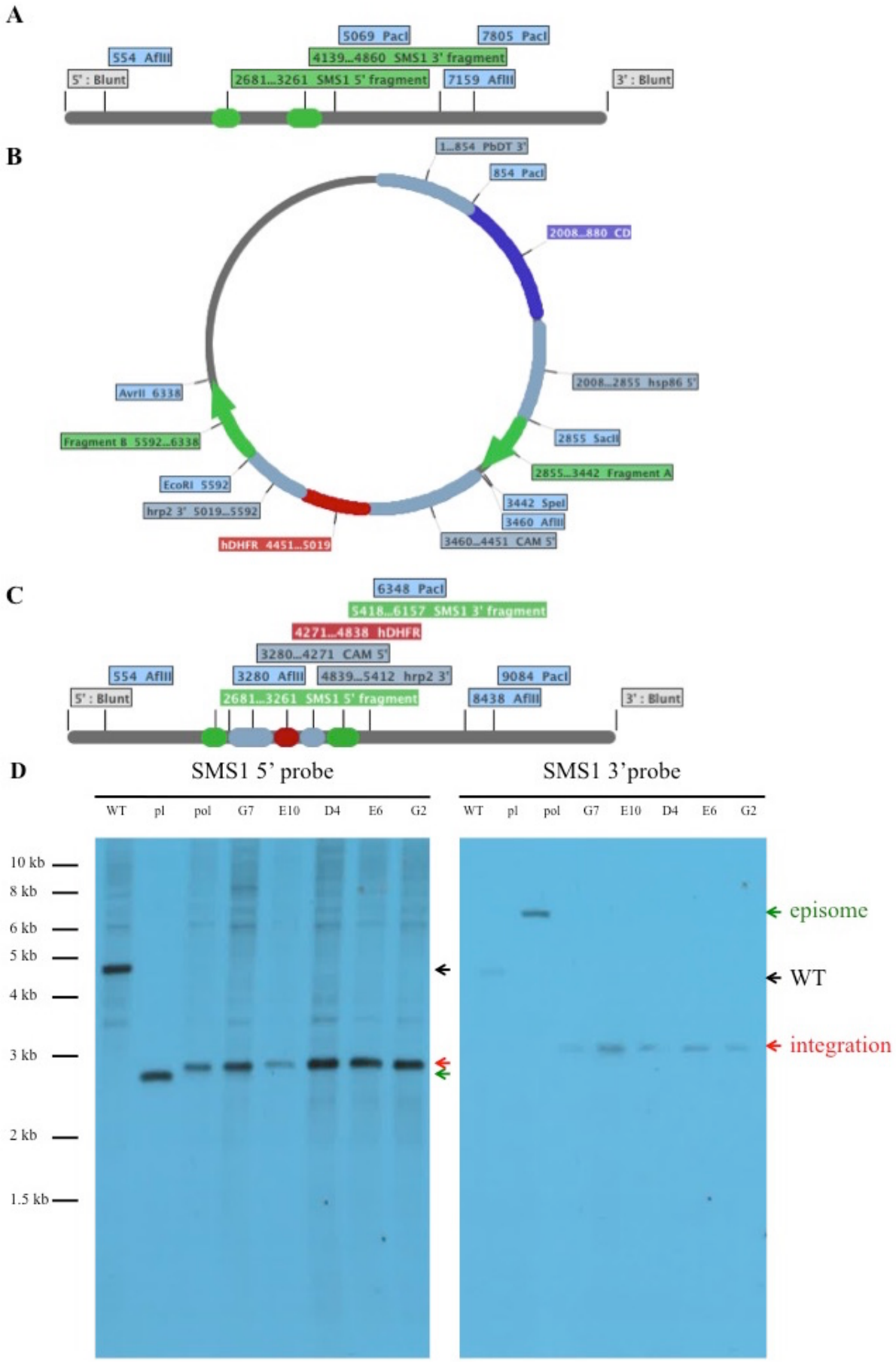

1

Fig. S1. Disruption of SMS1 by homologous recombination. A-C) Schematic of WT SMS1 locus with surrounding fragment of genomic DNA (A), pCC-1/SMS1 plasmid (B) and disrupted SMS1 locus with surrounding fragment of genomic DNA (C). SMS1 gene is disrupted by double homologous recombination at the 5' and 3' extremities of the gene in green (SMS1 5' fragment between SacII and SpeI restriction sites and SMS1 3' fragment between EcroRI and AvrII restriction sites), which inserts positive selection marker human dihydrofolate reductase (hDHFR, red) under the control of the calmodulin promoter (CAM 5') and histidine rich protein 2 3' untranslated region (hrp2 3'). The plasmid also contains negative selection maker cytosine deaminase (CD, purple) under the control of heat shock protein 86 promoter (hsp86 5') and *P. berghei* dihydrofolate reductase 3' untranslated region (PbDT 3') that are lost by double recombination. AflII and PacI restriction digest sites used for Southern blot are also indicated. D) Southern blot showing disruption of SMS1 locus. DNA from 3D7 wild type (WT), SMS1 KO plasmid (pl), polyclonal 3D7 transfected with SMS1 KO plasmid (pol) or clonal 3D7 transfected with SMS1 KO plasmid (G7, E10, D4, E6, G2) digested with AflII and PacI restriction enzymes and probed with 5' homologous flank probe (SMS1 5' probe, left) or 3' homologous flank probe (SMS1 3' probe, right). Expected SMS1 5' probe band lengths: WT locus: 4,515 bp (black arrow), episomal locus: 2,606 bp (green arrow), integrated locus: 2,726 bp (red arrow). Expected SMS1 3' probe band lengths: WT 2 locus: 4,515 bp (black arrow), episomal locus: 6,243 bp (green arrow), integrated locus: 3,068 bp (red arrow).

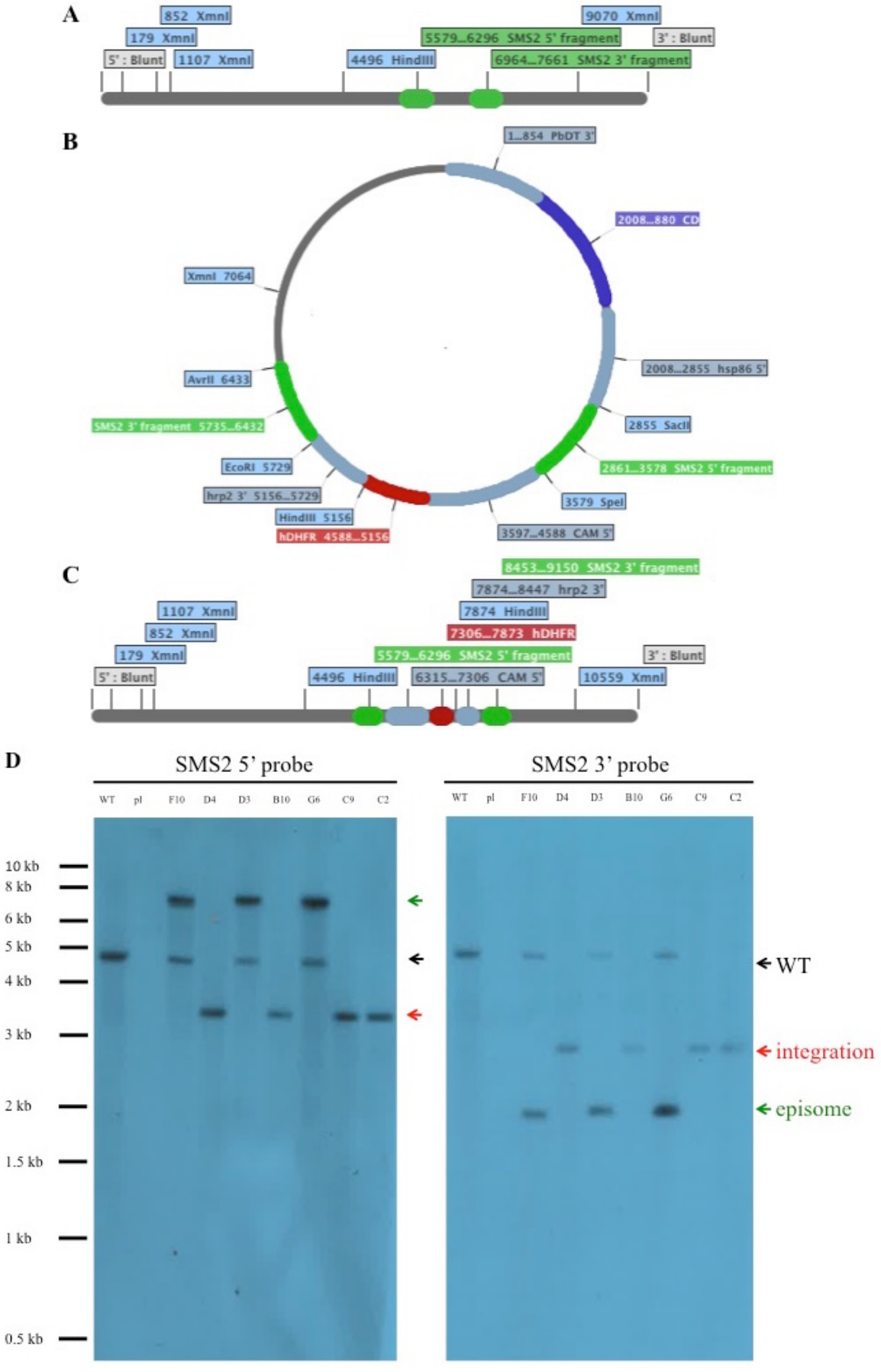

Fig. S2. Disruption of SMS2 by homologous recombination. A-C) Schematic of WT SMS2 locus with surrounding fragment of genomic DNA (A), pCC-1/SMS2 plasmid (B) and disrupted SMS2 locus with surrounding fragment of genomic DNA (C). SMS2 gene is disrupted by double homologous recombination at the 5' and 3' extremities of the gene in green (SMS2 5' fragment between SacII and SpeI restriction sites and SMS2 3' fragment between EcroRI and AvrII restriction sites), which inserts positive selection marker human dihydrofolate reductase (hDHFR, red) under the control of the calmodulin promoter (CAM 5') and histidine rich protein 2 3' untranslated region (hrp2 3'). The plasmid also contains negative selection maker cytosine deaminase (CD, purple) under the control of heat shock protein 86 promoter (hsp86 5') and *P. berghei* dihydrofolate reductase 3' untranslated region (PbDT 3') that are lost by double recombination. XmnI and HindIII restriction digest sites used for Southern blot are also indicated. D) Southern blot showing disruption of SMS2 locus. DNA from 3D7 wild type (WT), SMS2 KO plasmid (pl), or clonal 3D7 transfected with SMS2 KO plasmid (G7, E10, D4, E6 and G2) digested with XmnI and Hind III restriction enzymes probed with 5' homologous flank probe (SMS2 5' probe, left) or 3' homologous flank probe (SMS2 3' probe, right). Expected SMS2 5' probe band lengths: WT locus: 4,574 bp (black arrow), episomal locus: 7,036 bp (green arrow), integrated locus: 3,378 bp (red arrow). Expected SMS2 5' probe band lengths: WT locus: 4,574 bp (black arrow), episomal locus: 1,908 bp (green arrow), integrated locus: 2,685 bp (red arrow).

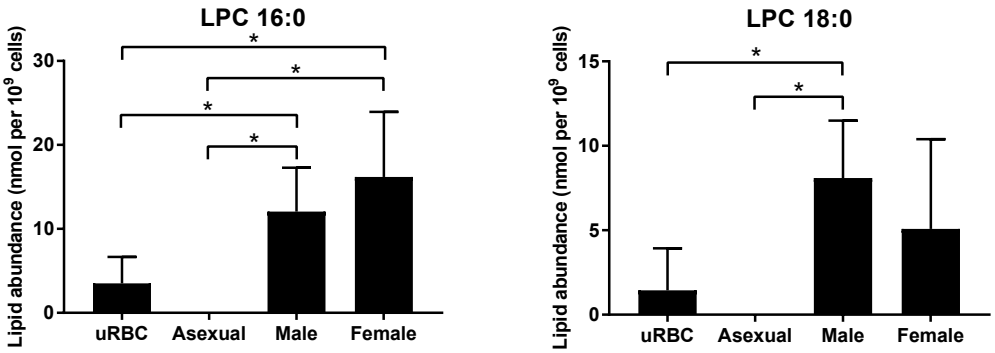

Fig. S3. Abundance of lysophosphatidylcholine (LPC) 16:0 (left) and LPC 18:0 (right) in uninfected red blood cells (uRBC) and red blood cells infected with asexual stage parasites (Asexual), male gametocytes (Male) or female gametocytes (Female) with results from student t tests (*: $p<0.1$; nothing indicated where $p>0.1$).

Table S1. Primers for construct preparation. Lowercase letters in the primer sequences correspond to restriction enzyme sites while uppercase letters refer to the gene sequence.

Primer code	Primer description		Primer sequence
al398	SMS1 5'	forward	atcccgcggCACACATTTGTACCTCTC
al399		reverse	gatactagtATCTGAGAAATTGGAACGC
al400	SMS1 3'	forward	atcgaattcGCTGCAAGAAGATATGC
al401		reverse	gatcctaggAAAAAGAGTTTGTAGGTG
al406	SMS2 5'	forward	atcccgcggGTTTAATACACGTGAG
al407		reverse	gatactagtCGATCACTTAATGGTTGCG
al408	SMS2 3'	forward	atcgaattcTATACCTTAGATTATGCC
al409		reverse	gatcctaggAAAAAACGACATTTAGGG

Table S2. Fitness competition primers to quantify wild type (SMS1 or SMS2 "cut out") and knock out (hDHFR) parasite genotype abundance relative to total parasite abundance (reference).

Target	Gene ID	Primers (forward/reverse)
SMS1 "cut out"	PF3D7_0625000	ACTGTTGATGTGTTAATGGGATATG ATCTTCTTGCAGCTACATCTACTA
SMS2 "cut out"	PF3D7_0625100	TTCATGCAAAGCCATTCTTTCT TGGCATAATCTAAGGTATAATTCAATCC
hDHFR		GAACTCAAGGAACCTCCACAA ACAGAACTGCCACCAACTATC
Reference	PF3D7_0317300	AATAGTCGAAGCGGGAAGTG CGAATTGGATTCTCCCAAATAACC

Table S3. Primers for Southern blot probe synthesis

Primer code	Primer description		Primer sequence
al 514	SMS1 5'	forward	CACACATTTGTACCTCTCTTA
al515		reverse	CCTTATGGTTGTAATGTTTGTC
al516	SMS1 3'	forward	TCACAGACAGATTCCAAGTGTT
al517		reverse	GGTACCATTTCCAGCGTATGA
al518	SMS2 5'	forward	GTAAATTAAAGACATGCACGTGAGA
al519		reverse	CGCTATCTGTTACTGACTCTTCAT
al520	SMS2 3'	forward	ACCCATAACAGAGGATAA
al521		reverse	ACGACATTTAGGGATTAAA

Table S4. List of detected lipid species other than free cholesterol in *P. falciparum*. CE: cholesteryl ester; DAG: diacylglycerol; TAG: triacylglycerol; LPC: lyso-phosphatidylcholine; PC: phosphatidylcholine; PE: phosphatidylethanolamine; PG: phosphatidylglycerol; PS: phosphatidylserine; Cer: ceramide; DHSM: dihydrosphingomyelin; SM: sphingomyelin.

Neutral Lipids		
CE 16:0	DAG (34:0) 16:0_18:0	TAG 52:1
CE 16:1	DAG (34:1) 16:0_18:1	TAG 52:2
CE 18:1	DAG (36:1) 18:0_18:1	TAG 52:3
CE 18:2	DAG (36:2) 18:1_18:1	TAG 54:2
CE 18:3	TAG 48:0	TAG 54:3
CE 20:4	TAG 50:0	TAG 54:6
CE 20:5	TAG 50:1	TAG 56:6
DAG (32:0) 16:0_16:0	TAG 50:2	

Phospholipids		
LPC 16:0	PC 38:7	PE 38:4
LPC 18:0	PC 40:4	PE 38:5
PC 32:0	PC 40:5	PE 38:6
PC 32:1	PC 40:6	PE 40:5
PC 34:0	PC 40:7	PE 40:6
PC 34:1	PC O-32:0	PG (34:1) 16:0_18:1
PC 34:2	PC O-34:1	PG (34:2) 16:0_18:2
PC 34:3	PC O-36:2	PG (36:1) 18:0_18:1
PC 36:0	PC O-38:4	PG (36:2) 18:0_18:2
PC 36:1	PC O-38:5	PG (36:2) 18:1_18:1
PC 36:2	PE 34:1	PG (36:3) 18:1_18:2
PC 36:3	PE 34:2	PS 34:1
PC 36:4	PE 36:1	PS 36:1
PC 36:5	PE 36:2	PS 36:2
PC 38:3	PE 36:3	PS 38:4
PC 38:4	PE 36:4	PS 38:5
PC 38:5	PE 36:5	PS 40:5
PC 38:6	PE 38:3	PS 40:6

Sphingolipids		
Cer 16:0	DHSM 25:0	SM 22:2
Cer 18:0	SM 14:0	SM 23:0
Cer 19:0	SM 15:0	SM 23:1
Cer 22:0	SM 16:0	SM 24:0
Cer 24:0	SM 16:1	SM 24:1
Cer 24:1	SM 17:0	SM 24:2
Cer 24:2	SM 18:0	SM 24:3
DHSM 16:0	SM 18:1	SM 25:0
DHSM 17:0	SM 19:0	SM 25:1
DHSM 18:0	SM 20:0	SM 26:0
DHSM 19:0	SM 20:1	SM 26:1
DHSM 20:0	SM 21:0	SM 26:2
DHSM 22:0	SM 22:0	
DHSM 24:0	SM 22:1	